Bergen ISSN 0803-2696/2001-06, CERN–TH/2001-322, Snowmass P3-42, hep-ph/0112312

Indirect Investigations of Supersymmetry

Gerald Eigen*
Department of Physics, University of Bergen, Allegaten 55, 5007 Bergen, Norway

Rick Gaitskell†
Department of Physics, Brown University, Providence, RI 02912, USA

Graham D. Kribs‡
Department of Physics, University of Wisconsin, Madison, WI 53706-1390, USA

Konstantin T. Matchev§
Theory Division, CERN, CH–1211, Geneva 23, Switzerland
(Dated: December 21, 2001)

This is the summary report of the "Indirect Investigations of SUSY" subgroup of the P3 Physics Group at Snowmass 2001.

I. INTRODUCTION

In this report we consider indirect probes of supersymmetry (SUSY). Following our charge, we will review the current experimental status and discuss possible levels of improvements in various measurements sensitive to supersymmetry through either virtual or astrophysics effects. We mention the upcoming experiments which are likely to achieve such precision, and outline which theoretical models and ideas can be tested by those experiments.

Since it is impossible to give a detailed review of every single topic here, we have limited our discussion to a few representative topics which were studied either at Snowmass or since then. A large fraction of this report is based on the individual written contributions [1, 2, 3, 4, 5, 6] to our subgroup as well as talks presented at Snowmass.

In Section II we discuss the implications of the recent $g_\mu - 2$ measurement (and its possible improvements) for supersymmetry. In Section III we review searches for *CP* violation and Section IV deals with lepton-flavor violation (LFV). Section V is devoted to the future of B-physics. In Section VI (VII) we discuss direct (indirect) searches for supersymmetric dark matter. We summarize and present our conclusions in Section VIII.

II. ANOMALOUS MAGNETIC MOMENT OF THE MUON

Undoubtedly, among the most exciting news of the year was the announcement of the new measurement of the muon anomaly at Brookhaven [7]. The muon anomalous magnetic moment a_μ was reported[1] to differ from the Standard Model (SM) prediction by 2.6σ

$$a_\mu^{\rm exp} - a_\mu^{\rm SM} = (43 \pm 16) \times 10^{-10} \ , \tag{1}$$

which is about three times larger than the Standard Model's electroweak contribution [16]. Deviations of roughly this order are expected in many models motivated by attempts to understand electroweak symmetry breaking. A supersymmetric interpretation is particularly attractive, since supersymmetry naturally provides electroweak scale contributions that are easily enhanced (by large $\tan\beta$) to produce deviations of the required magnitude. In addition, a_μ is both flavor- and *CP* -conserving. Thus, while the impact of supersymmetry on other low

*Gerald.Eigen@fi.uib.no
†gaitskell@physics.brown.edu
‡kribs@pheno.physics.wisc.edu
§Konstantin.Matchev@cern.ch

[1] Notice the recent questioning of the sign of the theoretical prediction for the light-by-light scattering contribution [8, 9]. With a consensus currently building towards the opposite sign [10, 11, 12], the deviation is less than 2σ. The purely hadronic contribution has also been under active discussion [13, 14, 15].

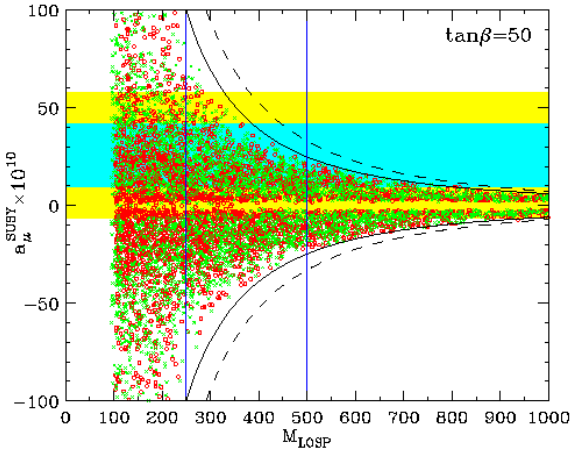

FIG. 1: Allowed values of $M_{\rm LOSP}$, the mass of the lightest observable supersymmetric particle (LOSP), and $a_\mu^{\rm SUSY}$ from a scan of parameter space with $M_1 = M_2/2$, $A_\mu = 0$, and $\tan\beta = 50$. Green crosses (red circles) have smuons (charginos/neutralinos) as the LOSP. A stable lightest supersymmetric particle (LSP) is assumed. Relaxing the relation $M_1 = M_2/2$ leads to the solid envelope curve, and further allowing arbitrary left-right smuon mixing (large A_μ) leads to the dashed curve. The envelope contours scale linearly with $\tan\beta$. The 1σ (dark shaded, blue) and 2σ (light shaded, yellow) allowed $a_\mu^{\rm SUSY}$ ranges are shown, and the discovery reaches of linear colliders with $\sqrt{s} = 500$ GeV and 1 TeV are given by the vertical blue lines. (From Ref. [2].)

energy observables (see sections III and IV) can be highly suppressed by scalar degeneracy or small *CP*-violating phases, supersymmetric contributions to a_μ are generic.

Supersymmetric contributions to a_μ have been explored for many years [17, 18, 19, 20, 21, 22, 23, 24, 25, 26]. Following the recent a_μ result, the implications for supersymmetry have been considered in numerous studies [27, 28, 29, 30, 31, 32, 33, 34, 35, 36, 37, 38, 39, 40, 41, 42, 43, 44, 45, 46, 47, 48, 49, 50, 51, 52]. The most significant consequence is that at least two superpartners cannot decouple, if supersymmetry is to explain the deviation, and one of these must be charged and so observable at colliders. Non-vanishing $a_\mu^{\rm SUSY}$ thus imply upper bounds on the mass $M_{\rm LOSP}$ of the lightest observable superpartner.

Fig. 1 shows the results from a series of high statistics scans in the relevant supersymmetric parameter space, consistent with slepton-flavor conservation: M_1, M_2, μ, $\tan\beta$, $m_{\tilde{\mu}_L}$, $m_{\tilde{\mu}_R}$, and A_μ. (For more details, see Ref. [27].) The points are obtained by assuming gaugino mass unification $M_1 = M_2/2$, fixing $A_\mu = 0$ and $\tan\beta = 50$, and scanning over the remaining parameters up to 2.5 TeV. Collider bounds from supersymmetry searches are enforced and a neutral LSP is assumed. Relaxing the gaugino unification assumption leads to possibilities bounded by the solid curve. Finally, allowing any A_μ in the interval $[-100\ {\rm TeV}, 100\ {\rm TeV}]$ extends the envelope curve to the dashed contour of Fig. 1. The envelope contours scale linearly with $\tan\beta$ to excellent approximation.

From Fig. 1 we see that the measured deviation in a_μ is in the range accessible to supersymmetric theories and is easily explained by supersymmetric effects. The case where the LSP decays visibly in collider detectors yields even lower bounds, and is examined in Ref. [27].

Such model-independent upper bounds have many implications. They improve the prospects for observation of weakly-interacting superpartners at the Tevatron and LHC. They also impact linear colliders: for reference, the discovery reach of linear colliders with $\sqrt{s} = 500$ GeV and 1 TeV are given in Fig. 1. In this highly model-independent framework, an observable supersymmetry signal is very probable at a 1.2 TeV linear collider; the expected improvements in a_μ measurements may significantly strengthen such conclusions. (The ultimate target of the BNL experiment is an experimental error of 4×10^{-10}.) Finally, these bounds provide fresh impetus for searches for lepton-flavor violation, which is also mediated by sleptons and charginos/neutralinos [45, 53].

Turning now to specific models, we first consider the framework of minimal supergravity, which is completely specified by four continuous parameters and one binary choice: m_0, $M_{1/2}$, A_0, $\tan\beta$, and $\mathrm{sign}(\mu)$. The first three are the universal scalar, gaugino, and trilinear coupling masses at the grand unified theory scale $M_{\rm GUT} \simeq 2 \times 10^{16}$ GeV.

In minimal supergravity (mSUGRA), $\mathrm{sign}(a_\mu^{\rm SUSY}) = \mathrm{sign}(\mu M_{1,2})$, so the a_μ result prefers a particular sign of μ relative to the gaugino masses. As is well-known, however, the sign of μ also enters in the supersymmetric contributions to $B \to X_s\gamma$. Current constraints on $B \to X_s\gamma$ require $\mu M_3 > 0$ if $\tan\beta$ is large (here M_3 is the gluino mass parameter). Gaugino mass unification implies $M_{1,2}M_3 > 0$, therefore, a large discrepancy in a_μ is

only possible for $a_\mu^{\rm SUSY} > 0$, in accord with the new measurement. Minimal supergravity, and gaugino unified models, in general, are generally consistent with the BNL measurement [27, 30, 31, 34, 35, 38, 42, 50, 54].

In contrast, the minimal model of anomaly-mediated supersymmetry breaking seems to be disfavored. One of the most striking predictions of anomaly mediation is that the gaugino masses are proportional to the corresponding beta function coefficients, and so $M_{1,2}M_3 < 0$. Anomaly-mediation, therefore, most naturally predicts $a_\mu^{\rm SUSY} < 0$ [55, 56], in contrast to the observed deviation. The dependence of this argument on the characteristic gaugino mass relations of anomaly mediation suggests that similar conclusions will remain valid beyond the minimal model.

In summary, the recently reported deviation in a_μ is easily accommodated in supersymmetric models. Its value provides *model-independent* upper bounds on masses of observable superpartners and already discriminates between well-motivated models.

III. *CP* VIOLATION

CP violation is among the least understood phenomena in the Standard Model. At present, *CP* violation is observed in only a small number of processes, such as in Kaon and B-meson mixing and decays. This can be accommodated through the single phase that appears in the CKM matrix. However, the CKM phase is not the only parameter that can lead to *CP* violation in the SM. The QCD θ term,

$$\theta \frac{g_3^2}{32\pi^2} G\tilde{G} \ , \tag{2}$$

where G is the gluon field strength and $\tilde{G}$ is its dual, also leads to *CP* violation, and indeed there are very strong constraints on this from limits on the electric dipole moment of the neutron (and mercury). Furthermore, *CP* violation is an essential ingredient of almost all attempts to explain the matter-antimatter asymmetry of the universe [57], yet the amount of *CP* violation present in the CKM matrix is insufficient to explain the observed asymmetry [58, 59, 60, 61]. Hence, searches for *CP* violation beyond the CKM matrix are an important probe into physics beyond the Standard Model.

Electric dipole moments (EDMs) violate both parity (P) and time reversal (T) invariance. If *CPT* is assumed to be an unbroken symmetry, a permanent EDM is, then, a signature of *CP* violation. A non-vanishing permanent EDM has not been measured for any of the known elementary particles. In the Standard Model, EDMs are generated only at the multi-loop level and are predicted to be many orders of magnitude below the sensitivity of foreseeable experiments [62, 63]. A non-vanishing EDM, therefore, would be unambiguous evidence for *CP* violation beyond the CKM matrix, and searches for permanent EDMs of fundamental particles are powerful probes of extensions of the Standard Model. In fact, current EDM bounds are already some of the most stringent constraints on new physics, and they are highly complementary to many other low energy constraints, since they require *CP* violation, but not flavor violation. In this Section we review the experimental prospects for the EDMs of various systems, and the implications for supersymmetry.

A. Experimental limits on EDMs

First, we summarize the current experimental bounds on EDMs and briefly mention future prospects. For the electron EDM, the current bound is [64]

$$d_e < 4 \times 10^{-27} \ e \ {\rm cm} \ , \tag{3}$$

although a new result was recently informally announced, $d_e < 1.5 \times 10^{-27}$ e cm [65]. It is unlikely significant further improvements can be expected due to stray magnetic fields. A new approach for the electron is a YbF molecule method [66] that could allow getting down to the 10^{-30} level within a decade [67]. The best current bound with this method is about an order of magnitude weaker than the bound quoted above.

For the neutron EDM, the current bound is [68]

$$d_n < 6.3 \times 10^{-26} \ e \ {\rm cm} \ , \tag{4}$$

and the expectation is to strengthen the limit down to 10^{-26} by 2004 [67]. By 2012 the goal is to reach the $10^{-28} e$ cm level using a cryogenic apparatus.

For ^{199}Hg atom EDM (Schiff moment), the current bound is [69]

$$d_{Hg} < 2.1 \times 10^{-28} \ e \ {\rm cm} \ , \tag{5}$$

from a 2001 analysis. There may be hope to improve this by another factor of two, although the systematic errors will need to be carefully investigated.

B. Supersymmetric effects

In the most general flavor non-preserving MSSM, there are over 40 new complex phases [70]. New complex phases arise, for example, in the Higgs mixing mass μ, as well as in the soft SUSY-breaking terms in the Lagrangian: the trilinear scalar mixing masses, the bilinear Higgs mixing parameter, and the gaugino mass parameters. Not all of these phases are physical, however, and many may be removed by field redefinitions.

In a wide range of supersymmetric models, these *CP* phases are expected to be $\mathcal{O}(1)$ [71]. Phases of this size lead to an EDM of the electron, neutron, and mercury atom that are significantly larger that experimental bounds. There are several possible ways to avoid these experimental constraints, with varying degrees of simplicity and naturalness. One solution is to simply take the phases to be small, of order 10^{-3} is sufficient [72, 73]. Another possibility is to allow arbitrary phases, but push (at least some of) the sparticle masses to the multi-TeV region which suppresses the supersymmetric contribution [74, 75, 76, 77]. Embedding supersymmetry in a left-right symmetric framework can also suppress the phases [78]. Finally, it is possible that large phases are permitted due to cancellations that conspire to render the SUSY contributions to EDMs below the experimental limits [79, 80].

The dominant contributions to the lepton EDMs arise from the one-loop chargino and one-loop neutralino graphs. For the neutron EDM, important contributions also arise from one-loop gluino graphs and two-loop stop-top and sbottom-bottom graphs. The operators that contribute are the electric dipole operator

$$-\frac{i}{2}d_f\overline{\psi}\sigma_{\mu\nu}\gamma_5\psi F^{\mu\nu}\ , \tag{6}$$

the chromoelectric dipole operator

$$-\frac{i}{2}\tilde{d}^C\overline{q}\sigma_{\mu\nu}\gamma_5 t^a q G^{\mu\nu,a}\ , \tag{7}$$

and the purely gluonic dim-6 operator

$$-\frac{i}{6}\tilde{d}^G f_{\alpha\beta\gamma}G_{\alpha\mu\rho}G^{\rho}_{\beta\nu}G_{\gamma\lambda\sigma}\epsilon^{\mu\nu\lambda\sigma}\ . \tag{8}$$

In extracting the effects of the chromoelectric and the purely gluonic operators, one can use naive dimensional analysis to relate [81]

$$d_q^C = \frac{e}{4\pi}\tilde{d}_q^C\eta^C\ ,\ d_q^G = \frac{eM}{4\pi}\tilde{d}^G\eta^G\ , \tag{9}$$

where $\eta^C \simeq \eta^G \sim 3.4$ and $M = 1.19$ GeV is the chiral symmetry breaking scale. The neutron EDM d_n is estimated using the $SU(6)$ quark model [81] $d_n = (\frac{4}{3}d_d - \frac{1}{3}d_u)$. (For an update using QCD sum rules, see [82].)

The EDM of ^{199}Hg arises from the T-odd nucleon-nucleon interaction in supersymmetry [83], induced mainly from the color operators with light quarks. This interaction gives rise to an EDM of the mercury atom by inducing the Schiff moment of the mercury nucleus. The QCD uncertainties related to this calculation are actually smaller than for the case of the neutron EDM. This interaction can be calculated in terms of the MSSM phases, with the result that there are somewhat better limits using mercury EDM than the electron EDM [83].

In fact, using the combination of the electron, neutron, and mercury EDM constraints severely limits the size of phases in the MSSM. Although this cannot be done in general (due to the large number of parameters), some information can be gleaned from a more restricted, 15-parameter MSSM. If we do not require gaugino mass unification at the scale where the gauge couplings intersect, then there are two independent phases in the gaugino masses since one can be made real by a $U(1)_R$ rotation. The 15-parameter MSSM considered by Ref. [84] consists of the phases in M_1, M_3, A_d, A_u, A_e, A_t, and μ, as well as the real quantities $\tan\beta$, the gaugino masses, a common scalar trilinear coupling, $|\mu|$, and the sfermions masses $m_{\tilde{e}_R}, m_{\tilde{\mu}_R}$. These parameters were sampled using a Monte Carlo scan of nearly 10^9 sets of parameters, and the remaining solutions satisfying all collider bounds *plus* the three EDM constraints were found. The results are illustrated in Fig. 2, in which the bounds on the phases of μ, M_1, and M_3 are shown. Notice that the constraint on $\arg(\mu)$ is strengthened significantly as $\tan\beta$ is increased. Furthermore, while there are lightly populated diagonal bands in [$\arg(\mu)$,$\arg(M_{1,2})$] space representing cancellations between diagrams, these regions suffer from larger fine-tuning and/or are (borderline) excluded by the Higgs mass limit. Clearly the parameter space is rather strongly constrained when all experimental constraints are applied and some lower bound on fine-tuning is imposed.

Finally, it is interesting to note that the operator giving rise to the electron EDM is similar to the operator for $g-2$, and this similarity can be utilized to find relations between these phenomena. In particular, assuming the BNL discrepancy is explained by supersymmetry, the phase of the electric dipole operator of the electron can be shown to be less than 2×10^{-3} [53].

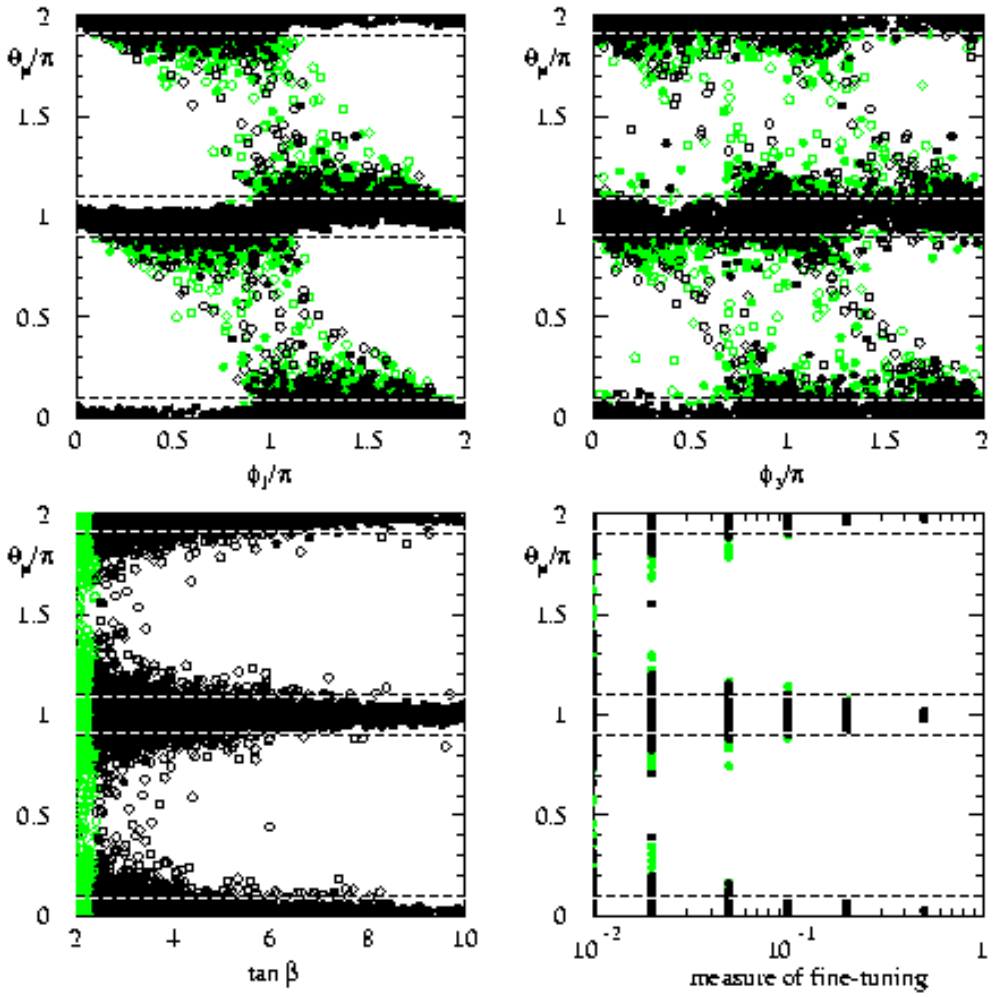

FIG. 2: Parameter sets in the 15-parameter MSSM satisfying the experimental limits on the electron, neutron, and mercury EDMs. The constraints on $\theta_\mu \equiv \arg(\mu)$ are the strongest, in comparison with $\phi_{1,3} \equiv \arg(M_{1,3})$. Open circles suffer from larger fine-tuning (< 0.01), defined by the maximum allowed variation of the input parameters such that the point survives the cuts. Lightly shaded (open or filled) circles have $m_h < 113$ GeV. (From Ref. [84].)

C. EDM of the Muon

The field of precision muon physics will be transformed in the next few years. The EDM of the muon d_μ is, therefore, of special interest. A new BNL experiment [85] has been proposed to measure the muon EDM at the level of

$$d_\mu \sim 10^{-24}\ e\ \text{cm}\ , \tag{10}$$

more than five orders of magnitude below the current bound [86]

$$d_\mu = (3.7 \pm 3.4) \times 10^{-19}\ e\ \text{cm}\ , \tag{11}$$

and even higher precision might be attainable at a future neutrino factory complex [87].

The interest in the muon EDM is further heightened by the recent measurement (1) of the muon magnetic-dipole moment (MDM) [7]. The EDM and MDM arise from similar operators, and this tentative evidence for a non-Standard Model contribution to a_μ also motivates the search for the muon EDM [88]. In fact, the deviation of Eq. (1) may be partially, or even entirely attributed to a muon EDM [88]! This is because in modern experiments the muon MDM is deduced by measuring (the magnitude of) the muon spin precession frequency in a perpendicular and uniform magnetic field. However, the spin precession frequency receives contributions from both the MDM and the EDM. For a muon traveling with velocity $\boldsymbol{\beta}$ perpendicular to both a magnetic

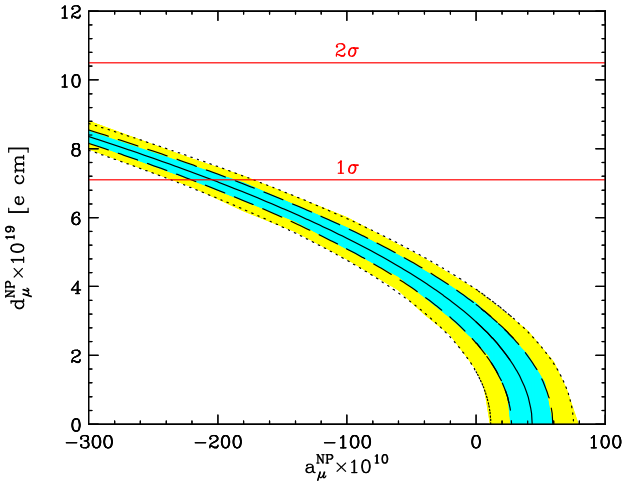

FIG. 3: Regions in the $(a_\mu^{\rm NP}, d_\mu^{\rm NP})$ plane that are consistent with the observed $|\,\boldsymbol{\omega}_a|$ at the 1σ and 2σ levels. The current 1σ and 2σ bounds on $d_\mu^{\rm NP}$ [86] are also shown. (From Ref. [1].)

field $\boldsymbol{B}$ and an electric field $\boldsymbol{E}$, the anomalous spin precession vector is

$$\boldsymbol{\omega}_a = -a_\mu \frac{e}{m_\mu}\,\boldsymbol{B} - d_\mu \frac{2c}{\hbar}\,\boldsymbol{\beta}\times\boldsymbol{B} - d_\mu \frac{2}{\hbar}\,\boldsymbol{E} - \frac{e}{m_\mu c}\left(\frac{1}{\gamma^2-1} - a_\mu\right)\boldsymbol{\beta}\times\boldsymbol{E}\ . \tag{12}$$

In recent experiments, the last term is removed by running at the 'magic' $\gamma \approx 29.3$, and the third term is negligible. For highly relativistic muons with $|\,\boldsymbol{\beta}\,| \approx 1$, then, the anomalous precession frequency is found from

$$\frac{|\,\boldsymbol{\omega}_a|}{|\,\boldsymbol{B}\,|} \approx \left[\left(\frac{e}{m_\mu}\right)^2 \left(a_\mu^{\rm SM} + a_\mu^{\rm NP}\right)^2 + \left(\frac{2c}{\hbar}\right)^2 d_\mu^{\rm NP\,2}\right]^{1/2}\ , \tag{13}$$

where NP (SM) denotes new physics (Standard Model) contributions, and assuming $d_\mu^{\rm NP} \gg d_\mu^{\rm SM}$.

We see that the effect (1) can also be due to a combination of new physics MDM and EDM contributions. Fig. 3 shows the regions in the $(a_\mu^{\rm NP}, d_\mu^{\rm NP})$ plane that are consistent with the observed deviation in $|\,\boldsymbol{\omega}_a|$. The current 1σ and 2σ upper bounds on $d_\mu^{\rm NP}$ [86] are also given. It is evident from the figure that a large fraction of the region allowed by both the current a_μ measurement (1) and the d_μ bound (11) is already within the sensitivity of phase I of the newly proposed experiment (with sensitivity $\sim 10^{-22}$ e cm).

The proposed dedicated muon EDM experiment will use a different setup, by applying a constant radial electric field. In that case a similar EDM $\leftrightarrow$ MDM ambiguity is present [1], and can be resolved by up-down asymmetry measurements.

It is useful to write the new physics contributions to the EDM and MDM operators as

$$d_\mu^{\rm NP} = \frac{e}{2m_\mu}\,\mathcal{I}mA\ , \qquad\qquad a_\mu^{\rm NP} = \mathcal{R}eA\ , \tag{14}$$

with $A \equiv |A|e^{i\phi_{\rm CP}}$. This defines an experimentally measurable quantity $\phi_{\rm CP}$ which quantifies the amount of *CP* violation in the new physics, independently of its energy scale. Upon eliminating $|A|$, one finds

$$d_\mu^{\rm NP} = 4.0\times10^{-22}\ e\ {\rm cm}\ \frac{a_\mu^{\rm NP}}{43\times10^{-10}}\ \tan\phi_{\rm CP}\ . \tag{15}$$

The measured discrepancy in $|\,\boldsymbol{\omega}_a|$ then constrains $\phi_{\rm CP}$ and $d_\mu^{\rm NP}$. The preferred regions of the $(\phi_{\rm CP}, d_\mu^{\rm NP})$ plane are shown in Fig. 4. For 'natural' values of $\phi_{\rm CP} \sim 1$, $d_\mu^{\rm NP}$ is of order 10^{-22} e cm. With the proposed $d_\mu^{\rm NP}$ sensitivity of (10), all of the 2σ allowed region with $\phi_{\rm CP} > 10^{-2}$ r yields an observable signal.

At the same time, while this model-independent analysis indicates that natural values of $\phi_{\rm CP}$ prefer $d_\mu^{\rm NP}$ well within reach of the proposed muon EDM experiment, very large values of $d_\mu^{\rm NP}$ also require highly fine-tuned $\phi_{\rm CP}$. For example, we see from Fig. 4 that values of $d_\mu^{\rm NP} \gtrsim 10^{-20}$ e cm are possible only if $|\pi/2 - \phi_{\rm CP}| \sim 10^{-3}$. Furthermore, in specific supersymmetric models it is difficult to achieve values of d_μ large enough to affect the conventional interpretation of (1). For example, in supersymmetry, assuming flavor conservation and taking

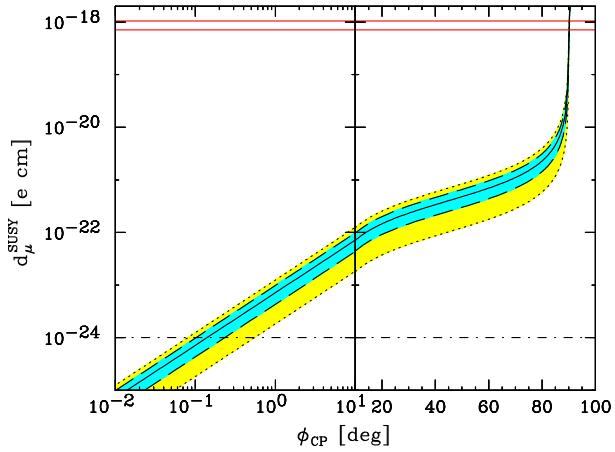

FIG. 4: Regions of the $(\phi_{\rm CP}, d_\mu^{\rm NP})$ plane allowed by the measured central value of $|\,\boldsymbol{\omega}_a|$ (solid) and its 1σ and 2σ preferred values (shaded). The horizontal dot-dashed line marks the proposed experimental sensitivity to $d_\mu^{\rm NP}$. The red horizontal solid lines denote the current 1σ and 2σ bounds on $d_\mu^{\rm NP}$ [86]. (From Ref. [1].)

extreme values of sparticle masses ($\sim$ 100 GeV) and $\tan\beta$ ($\tan\beta \sim 50$) to maximize the effect, the largest possible value of a_μ is $a_\mu^{\rm max} \sim 10^{-7}$ [27]. Very roughly, one therefore expects a maximal d_μ only of order $(e\hbar/2m_\mu c)a_\mu^{\rm max} \sim 10^{-20}$ e cm in supersymmetry. Similar conclusions hold for specific models as well [89].

Simplest models relate the EDMs of the electron and muon by 'naive scaling':

$$d_\mu \approx \frac{m_\mu}{m_e}\, d_e \ . \tag{16}$$

Given the current published bound on the electron EDM, 'naive scaling' limits the muon EDM as

$$d_\mu \lesssim 9.1 \times 10^{-25}\ e \text{ cm} \ , \tag{17}$$

at the 90% CL, barely below the sensitivity of (10). Naive scaling must be violated if a non-vanishing d_μ is to be observable at the proposed experiment, and this may happen in one of three ways:

- Departure from scalar degeneracy, *i.e.* generation-dependent slepton masses [88].
- Departure from proportionality, *i.e.* the A terms do not scale with the corresponding fermion mass [90].
- Flavor violation, *i.e.* non-vanishing flavor off-diagonal elements for the sfermion masses and the A-terms [53, 88].

Such multitude of possibilities provides sufficient motivation and relatively good prospects for a dedicated muon EDM experiment.

IV. LEPTON FLAVOR VIOLATION

One of the most powerful probes of low energy supersymmetry are the precise measurements and limits on flavor-violating processes. In the squark sector, for example, the smallness of $K_0 \leftrightarrow \overline{K}_0$ mixing either requires tiny off-diagonal squark (mass)^2 elements, or pushes supersymmetry to embarrassingly high scales $\sim \mathcal{O}(100\,\text{TeV})$ [91, 92, 93]. Similarly strong constraints are also present for certain elements in the slepton mass matrix. Here, we discuss a few of the strongest constraints from limits on rare $\mu \to e$ processes.

A. Experimental status

There are also several experimental probes that tightly constrain lepton-flavor violation. The strongest constraints arise from the rare $\mu \to e$ processes: $\mu \to e\gamma$, $\mu \to 3e$, and $\mu \to e$ conversion. The current bounds

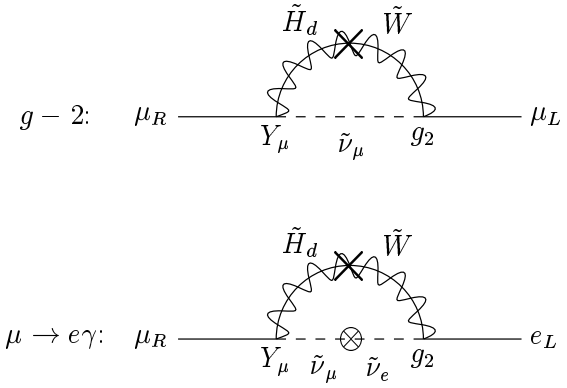

FIG. 5: One example set of chargino-sneutrino contributions to muon $g-2$ and $\mu \to e\gamma$ in the interaction eigenstate basis with incoming right-handed muons. The photon (not shown) is emitted from the chargino. The chirality flip is shown by the $\times$ on the fermion line, while the the lepton flavor violating mass insertion is shown by the $\otimes$. (From Ref. [45].)

on these processes are

$$\begin{aligned} BR(\mu \to e\gamma) &< 1.2 \times 10^{-11} \text{ [94]} \\ BR(\mu \to 3e) &< 1.0 \times 10^{-12} \text{ [95]} \\ BR(\mu \to e \text{ conversion}) &\lesssim 2 \times 10^{-12} \text{ [96]} , \end{aligned}$$

with the precise bound on $\mu \to e$ conversion dependent on the particular host scattering nucleus.

Improvements to these bounds are on the horizon. At PSI, there is a proposal to improve the limit on $\mu \to e\gamma$ down to 10^{-14} [97], which is likely to get at least to the level of a few $\times 10^{-13}$, since PSI has a $\times 20$ advantage over LAMPF in duty cycle and the planned detector is probably at least as capable as that of MEGA (the previous experiment). This experiment could possibly be pursued further at BNL, since a very intense muon beam will be built for another experiment.

There is also a detailed proposal by MECO [98] to improve the limit on $\mu \to e$ conversion down to order 10^{-16} at the BNL AGS. No other facility can compete at the moment, but toward the end of the decade the Japanese Joint Project might get involved. There is apparently a plan to build a dedicated cooled muon beam there at an early stage, which they claim would make possible an experiment at the 10^{-18} level. Note that one can talk about such amazing sensitivity for this process because it has an excellent signature that does not require a coincidence and so is robust against high rates.

B. Supersymmetric contributions

Supersymmetric contributions to these processes dominantly arise when flavor violating contributions to the slepton mass matrix are present. The sizes of these flavor-violating elements of the slepton mass matrix are arbitrary in the MSSM. Particular models of supersymmetry breaking and mediation can in some cases predict the size of slepton-flavor violation. Some examples include supersymmetric unified theories (e.g., see [99]), and also exponentially suppressed contributions from sequestering [100, 101, 102].

The contributions to $\mu \to e\gamma$ are particularly interesting, due to the strong resemblance between the operators giving rise to muon $g-2$ and those giving $\mu \to e\gamma$ [45, 53]. This correspondence is best revealed diagrammatically. In particular, there is a precise correspondence between the diagrams that contribute to $\mu \to e\gamma$ (and $\tau \to \mu\gamma$) with those that contribute to the muon anomalous magnetic moment [45]. This is illustrated for one class of diagrams involving charginos and sneutrinos in Fig. 5. Other than emitting an electron instead of a muon, the contribution has the same form except for the essential addition of a sneutrino flavor-mixing mass insertion and a propagator for the electron sneutrino. Using just this process, is it easy to see that the amplitudes for $g-2$ and $\mu \to e\gamma$ are related by

$$a_{\mu \to e\gamma} = \frac{m^2_{e\mu}}{m^2_{\tilde{\nu}_e}} a_\mu \tag{18}$$

in the mass-insertion approximation, assuming for this example $m_{\tilde{\nu}_e} > m_{\tilde{\nu}_\mu}, m_{\tilde{\chi}^\pm}$. Here, $m^2_{e\mu}$ is the off-diagonal element in the sneutrino (mass)^2 matrix. One can systematically go through all classes of one-loop diagrams and all possible sparticle-mass hierarchies to find [45]

$$BR(\mu \to e\gamma) \simeq 10^{-4} \left(\frac{a_\mu}{4.3 \times 10^{-9}}\right)^2 \frac{m^2_{e\mu}}{\tilde{m}^2} \tag{19}$$

where $\tilde{m} = \mathrm{Max}[m_{\tilde{\chi}}, m_{\tilde{\ell}_e}]$ is the largest mass in the loop. So, if the deviation in the muon $g-2$ measured at the BNL experiment is interpreted as supersymmetry, we obtain strong model-independent bounds on the sfermion mass mixing,

$$m^2_{e\mu}/\tilde{m}^2 \;\leq\; 2 \times 10^{-4} \tag{20}$$

$$m^2_{\mu\tau}/\tilde{m}^2 \;\leq\; 0.1\ . \tag{21}$$

(The bounds on the "left-left" and "right-right" slepton masses are essentially the same, using the approach of [45].) The bound on the second-third generation mass mixing is much weaker due to the weaker limit on the decay $BR(\tau \to \mu\gamma) < 1.1 \times 10^{-6}$ [103]. These results are largely insensitive to any supersymmetric parameters. Indeed, for some mass ranges the bounds can be as much as an order of magnitude better than quoted above. The only assumption is that there are no accidental cancellations resulting from summing over diagrams, and even then the expectation is that the bounds are only mildly relaxed.

Finally, there are exciting prospects for directly observing slepton-flavor physics at a linear collider [104]. Even with a limited number of slepton states, the observation (or non-observation) of slepton-flavor violation is expected to provide important clues to the underlying supersymmetry breaking structure. The reason that observable sflavor violation at a LC is possible is easy to understand. In many proposals to solve the SUSY-flavor problem, a high degree of degeneracy among sleptons (and squarks) is predicted. As a result, there is the potential for substantial mixing of flavor eigenstates. This can lead to substantial and observable sflavor violation. To be readily observable, it is necessary that the mass splittings between the states not be too much smaller than the decay widths, and that the mixing angles not be terribly small. In the case when the off-diagonal mass terms are comparable or larger than the widths, dramatic collider signatures are possible (see, e.g., Ref. [105, 106, 107]).

V. B PHYSICS

Rare decays and *CP* violating asymmetries provide another interesting hunting ground for SUSY-mediated processes. In the B system many rare decays involve $b \to s(d)$ transitions, which are flavor-changing neutral-current (FCNC) processes that are forbidden in SM at tree level but occur at loop level. The one-loop processes involve gluonic, electromagnetic or weak penguin diagrams as well as box diagrams. Though suppressed in SM they are relatively large because of the CKM structure and the top-quark dominating the loop. However, SUSY processes may become competitive and interfere with those in SM. Depending on the sign of the interference term enhanced or depleted branching fractions are obtained. Due to the presence of new weak phases SUSY processes may affect *CP* asymmetries as well. While *CP* asymmetries of rare decays to flavor eigenstates are typically small in SM ($\leq 1\%$) enhancements up to 20% are possible in SUSY models. For *CP* asymmetries of B decays to *CP* eigenstates, which are quite sizable in SM, SUSY processes either may enhance or deplete the effect. Other interesting penguin modes are B^0_s and B^0_d decays into two charged leptons, which are highly suppressed in SM and, therefore, bear a high sensitivity for New Physics. To establish a coherent picture of B decays and uncover SUSY contributions it is important to perform several high-precision measurements of rare-decay branching fractions and *CP* asymmetries.

CLEO was the first experiment to observe and study FCNC B decays [108]. However, the CLEO data sample is limited to 9.1 fb^{-1}. At the asymmetric B factories, which started operation in 1999, BABAR and BELLE have recorded already data samples of 60 fb^{-1} and 44 fb^{-1}, respectively. By summer 2002, BABAR expects 100 fb^{-1}. This will be increased to 500 fb^{-1} by summer 2005. If luminosity upgrades are successful as planned each experiment should reach 1 ab^{-1} by 2010. Experiments at the Tevatron (CDF, D0) will augment B samples. However, starting 2006 high-precision measurements are expected from BTEV at the Tevatron and LHCb, ATLAS and CMS at the LHC. Furthermore, there are ongoing discussions about a super B factory operating with peak luminosities of 10^{36} cm^{-2}s^{-1}, which would deliver 10 ab^{-1} per year [6, 109]. Thus, high-statistics B samples should be available in the future. In the following we summarize expectations regarding radiative penguin decays [6], *CP* violation in B decays [109] and B decays into two charged leptons. Whenever possible, the extrapolations are based on present measurements.

A. Radiative Penguin Decays

Radiative penguin decays involve electroweak penguin loops or box diagrams. The largest decay is $B \to X_s\gamma$, which is dominated by the magnetic-dipole operator O_7. The SM decay rate contains the squares of the CKM matrix elements $\mid V_{ts} \mid$ and the Wilson coefficient C_7. The latter accounts for all perturbative QCD contributions. Due to operator mixing an effective Wilson coefficient results. The non-perturbative contributions are absorbed into the hadronic matrix element of the magnetic dipole operator. Because of large model uncertainties one avoids the calculation of the hadronic matrix element by using the approximation that the ratio of decay rates of $b \to s\gamma$ and $b \to ce\bar{\nu}$ at the parton level is equal to that at the meson level (quark-hadron duality). SUSY processes yield additional contributions C_7^{new} and C_8^{new}, where the latter arises from SUSY operators that are equivalent to the chromomagnetic dipole operator O_8.

The branching fraction in next-to-leading order (NLO) in SM is predicted to be $\mathcal{B}(B \to X_s\gamma) = (3.28 \pm 0.33) \times 10^{-4}$ [110]. Recently, however, Gambino and Misiak argued for a different choice of the charm-quark mass, which increases the branching fraction to $\mathcal{B}(B \to X_s\gamma) = (3.73 \pm 0.3) \times 10^{-4}$ [111]. The present theoretical uncertainty of $\sim 10\%$ is dominated by the mass ratio of the c-quark and b-quark and the choice of the scale parameter μ_b. In an updated analysis using the full sample of 9.1 fb^{-1} CLEO has measured $\mathcal{B}(B \to X_s\gamma) = (3.21 \pm 0.43_{(stat)} \pm 0.27_{(sys)}{}^{+0.18}_{-0.10\ (th)}) \times 10^{-4}$ [112], where the errors represent statistical, systematic, and theoretical uncertainties, respectively. Because of the large errors this is consistent with the SM NLO prediction. Note that the signal region is dominated by continuum (75%) and $B\bar{B}$ (12%) backgrounds which have to be subtracted. The present relative statistical error is 13.4%. Assuming that measurements improve with luminosity as $1/\sqrt{\mathcal{L}}$ the relative statistical error $\sigma_{\mathcal{B}}/\mathcal{B}$ will be reduced to 4% (1.3%) for luminosities of 100 fb^{-1} (1 ab^{-1}). In a super B factory one would expect $\sigma_{\mathcal{B}}/\mathcal{B} = 0.4\%$ for 10 ab^{-1}. The present relative systematic error is 8.4%. It is expected that with increased statistics the systematic error can be reduced substantially by using appropriate data selections and by improving measurements of the tracking efficiency, photon energy, photon efficiency and B counting. For 10 ab^{-1} the hope is to reach a systematic error of $1 - 2\%$.

The CLEO $\mathcal{B}(B \to X_s\gamma)$ measurement already provides a significant constraint on the SUSY parameter space. For example, the new physics contributions to $B \to X_s\gamma$, C_7^{new} and C_8^{new}, have been calculated using the minimal supergravity model (SUGRA) [113]. Many solutions have been generated by varying the input parameters within the ranges $0 < m_0 < 500$ GeV, $50 < m_{1/2} < 250$ GeV, $-3 < A_0/m_0 < 3$ and $2 < \tan\beta < 50$, where a common scalar mass m_0 for squarks and sleptons, a common gaugino mass $m_{1/2}$ and a common trilinear scalar coupling A_0 is assumed in SUGRA. As usual the ratio of vacuum expectation values of the neutral components of the two Higgs doublets is parameterized by $\tan\beta$. The top-quark mass was kept fixed at $m_t = 175$ GeV. Only solutions were retained that were not in violation with SLC/LEP constraints and Tevatron direct sparticle production limits. For these the ratios $R_7 = C_7^{new}(M_W)/C_7^{SM}(M_W)$ and $R_8 = C_8^{new}(M_W)/C_8^{SM}(M_W)$ were determined. The results are depicted in Figure 6 [114]. The solid bands show the regions allowed by the CLEO measurement. It is interesting to note that many solutions are already in conflict with the data. However, due to the theoretical uncertainties it will be difficult to uncover SUSY contributions at high luminosities, if the central value remains closely to the present result.

The exclusive decay rate for $B \to K^*\gamma$ involves the hadronic matrix element of the magnetic dipole operator, which in general is expressed in terms of three q^2-dependent form factors $T_i(q^2)$. For on-shell photons T_3 vanishes and T_2 is related to T_1. For the determination of the form factors various techniques are used, introducing additional theoretical uncertainties. Recently, two NLO calculations were carried out, predicting SM branching fractions of $\mathcal{B}(B \to K^*\gamma) = (7.1^{+2.5}_{-2.3}) \times 10^{-5}$ [115] and $\mathcal{B}(B \to K^*\gamma) = (7.9^{+3.5}_{-3.0}) \times 10^{-5}$ [116]. The most precise branching-fraction measurements of the exclusive decays $B^0 \to K^{*0}\gamma$ and $B^+ \to K^{*+}\gamma$ have been achieved by BABAR. Utilizing kinematic constraints in the B rest frame provides a substantial reduction of $q\bar{q}$-continuum background here. In a sample of 20.7 fb^{-1} BABAR measured $\mathcal{B}(B^0 \to K^{*0}\gamma) = (4.39 \pm 0.41 \pm 0.27) \times 10^{-5}$ in the $K^+\pi^-$ final state [117]. Due to the large theoretical errors of $35 - 40\%$ the BABAR measurement is still consistent with the NLO SM predictions. Note that the combined statistical and systematic error is already more than a factor of three smaller than the theoretical uncertainty. The precision expected for increased luminosities will be comparable to that in the inclusive mode. Thus, it will be difficult to use the exclusive modes for SUSY discoveries, unless the theoretical errors are considerably reduced or SUSY effects are gigantic. In hadron colliders $B \to K^{*0}\gamma$ is also measurable. CDF expects to achieve a 7.6% statistical error per 2 fb^{-1}, while BTEV [118] and LHCb [119] estimate a statistical error of $\sigma_{\mathcal{B}}/\mathcal{B} \sim 0.6\%$ per year of LHC running (~ 2 fb^{-1}).

Other interesting radiative penguin decays are the $B \to X_s\ell^+\ell^-$ modes, where $\ell^\pm$ is either an $e^\pm$ or a $\mu^\pm$. In SM, these decays are suppressed by about two orders of magnitude with respect to corresponding $B \to X_s\gamma$ modes. The suppression by α is compensated partially by additional contributions from the Z^0-penguin diagram and a box diagram that involves the semileptonic operators, O_{9V} and O_{10A}. Each of them can receive additional SUSY contributions. The branching fractions of the inclusive modes in SM in NLO are predicted to be $\mathcal{B}(B \to X_s e^+e^-) = (6.3^{+1.0}_{-0.9}) \times 10^{-6}$ and $\mathcal{B}(B \to X_s\mu^+\mu^-) = (5.7 \pm 0.8) \times 10^{-6}$ [120, 121, 122].

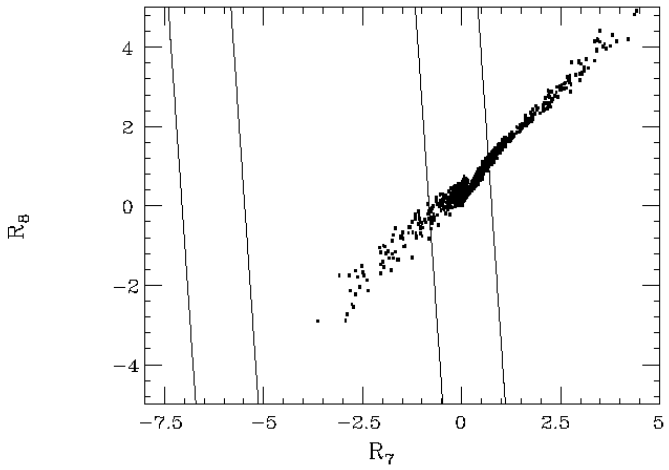

FIG. 6: Scatter plot of R_8 versus R_7 for solutions obtained in the SUGRA model. The region allowed by the CLEO measurement lies inside the two sets of solid diagonal bands.

The theoretical uncertainties are about 16%. These modes have not been observed so far. The lowest branching-fraction upper limits @90% from CLEO are about an order of magnitude above the SM predictions [123]. Using SM predictions and efficiencies determined by CLEO an observation of the $X_s e^+e^-$ and $X_s\mu^+\mu^-$ modes is expected in a sample of 100 fb^{-1} with statistical errors around $\sim 17\%$ and $\sim 19\%$, respectively. This will be improved to $\sim 5.3\%$ ($\sim 1.7\%$) and $\sim 6\%$ ($\sim 1.9\%$) in samples of 1 ab^{-1} (10 ab^{-1}), respectively. Unless the SUSY contributions lead to significant enhancements the theory errors need to be reduced at the same time precise measurements are obtained in order to increase the sensitivity for observing New Physics.

Branching fractions of the exclusive modes are further suppressed. Using SM predictions from two recent models and their uncertainties yield the following ranges of branching fractions: $\mathcal{B}(B \to K\ell^+\ell^-) = (4.7 - 7.5) \times 10^{-7}$, $\mathcal{B}(B \to K^* e^+e^-) = (1.4 - 3.0) \times 10^{-6}$, and $\mathcal{B}(B \to K^*\mu^+\mu^-) = (0.9 - 2.4) \times 10^{-6}$ [124, 125]. SUSY processes could enhance these branching fractions considerably. As an example Figure 7 depicts the dilepton-mass-squared spectrum for $B \to K^*\mu^+\mu^-$ calculated in SM, SUGRA models and minimal-insertion-approach SUSY models (MIA) [125]. Shown are both the pure penguin contribution and the sum of the penguin process and the long-distance effects, displaying constructive interference below the charmonium resonances and destructive interference above. The different models are characterized in terms of ratios of Wilson coefficients $R_i = 1 + C_i^{new}/C_i^{SM}$ for $i = 7, 9, 10$. The SM prediction is the lowest but bears large uncertainties.

Except for an unconfirmed signal in $B \to K^+\mu^+\mu^-$ seen by BELLE, none of the exclusive $B \to K(K^*)\ell^+\ell^-$ modes have been observed yet. The branching fraction of $\mathcal{B}(B \to K\mu^+\mu^-) = (0.99^{+0.40+0.13}_{-0.32-0.14}) \times 10^{-6}$ measured by BELLE [126] is barely consistent with the BABAR limit of $\mathcal{B}(B \to K\ell^+\ell^-) < 0.6 \times 10^{-6}$ @90% CL [117]. The BABAR limits of $\mathcal{B}(B \to K^{*0} e^+e^-) < 5.0 \times 10^{-6}$, and $\mathcal{B}(B \to K^{*0}\mu^+\mu^-) < 3.6 \times 10^{-6}$ [117] lie less than a factor of two above the SM predictions. In a sample of 100 fb^{-1} we expect first observation of these modes. The statistical errors expected at high luminosities for $B \to K^{*0}\ell^+\ell^-$ are about a factor of two higher than those for the corresponding inclusive modes. Experiments at the Tevatron and LHC will be competitive in the $K^{*0}\mu^+\mu^-$ and $K^+\mu^+\mu^-$ final states [118].

The lepton forward-backward asymmetry $\mathcal{A}_{fb}(s)$ as a function of $s = m^2_{\ell\ell}$ is an observable that is very sensitive to SUSY contributions. It reveals characteristic shapes in the SM both for inclusive and exclusive final states. To avoid complications from the charmonium resonances one restricts the range s to masses below the J/ψ, which accounts for $\sim 40\%$ of the entire spectrum. Figure 7 shows $\mathcal{A}_{fb}(s)$ for the $B \to K^{*0}\mu^+\mu^-$ mode [125]. In SM, the position s_0 of $\mathcal{A}_{fb}(s_0) = 0$ is predicted to lie at $s_0 = 2.88^{+0.44}_{-0.28}$ GeV^2. Both, the shape and s_0 are expected to differ significantly in New Physics models. The shape is very sensitive to the sign of R_7 and varies from model to model. Thus, a precise measurement of $\mathcal{A}_{fb}(q^2)$ may permit an extraction of the coefficients R_i. However, to achieve sufficient precision a super B factory is needed. For Measuring 18 data points below $s = 9$ GeV^2 with 100 events each in the $B \to X_s\ell^+\ell^-$ ($B \to K^{*0}\ell^+\ell^-$) modes at a super B factory (10 ab^{-1}/y) requires a run period of 0.3-0.4 (0.8-1.3) years. For comparison, LHCb expects to achieve the same precision in the $B \to K^{*0}\mu^+\mu^-$ mode in about one year.

The modes bearing the smallest theoretical uncertainties are the $B \to X_s\nu\bar{\nu}$ decays, since long distance

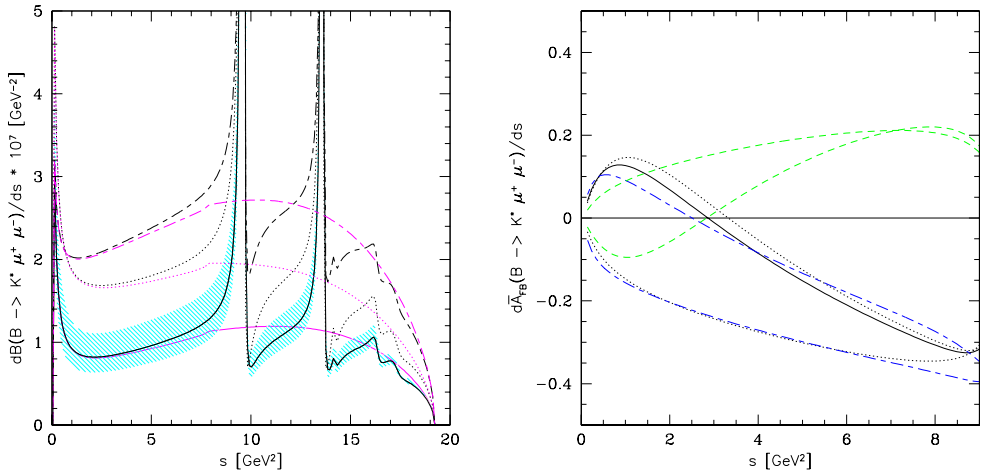

FIG. 7: The dilepton invariant mass-squared spectrum (left) and the normalized forward-backward asymmetry (right) as a function of $s = m^2_{\mu\mu}$ in $B \to K^*\mu^+\mu^-$ [125]. The solid lines denote the SM prediction. The shaded region depicts form-factor related uncertainties. The dotted lines correspond to a SUGRA model ($R_7 = -1.2, R_9 = 1.03, R_{10} = 1$) and the dash-dotted lines to a MIA model ($R_7 = -0.83, R_9 = 0.92, R_{10} = 1.61$). In the $m^2_{\mu\mu}$ spectrum both the penguin contribution and the distribution including long-distance effects are shown. In the $\mathcal{A}_{fb}$ plot the upper and lower sets of curves show the difference between $C_7^{(0)eff} < 0$ and $C_7^{(0)eff} > 0$, while the dashed curves give results for another MIA model ($R_7 = \mp 0.83, R_9 = 0.79, R_{10} = -0.38$).

effects are absent and QCD corrections are small. Here, only weak penguin and box diagrams contribute. However, experimentally both inclusive and exclusive modes are difficult to observe due to the two neutrinos. To reduce backgrounds from $q\bar{q}$ continuum and other B decays at least a partial reconstruction of the other B is necessary. Since branching fractions are slightly lower than those in the corresponding $B \to X_s\mu^+\mu^-$ channels [124, 127, 128, 129], several years of running at a super B factory (at 10^{36} cm^{-2}s^{-1}) are needed to study these modes. For example, in a sample of 10 ab^{-1} the relative statistical error expected in the inclusive $B \to X_s\nu\bar{\nu}$ branching fraction is $\sigma_{\mathcal{B}}/\mathcal{B} \sim 5\%$. For the $K^*\nu\bar{\nu}$ and $K\nu\bar{\nu}$ final states the relative statistical errors are $\sigma_{\mathcal{B}}/\mathcal{B} \sim 10\%$ and $\sigma_{\mathcal{B}}/\mathcal{B} \sim 13\%$, respectively [6].

B. *CP* Violation

CP violation can arise from different effects. We focus here on (i) *CP* violation resulting from the interference between decays with and without mixing, which occurs when decay rates of a B^0 and $\bar{B}^0$ into a *CP* eigenstate or into *CP*-conjugate states differ, and on (ii) *CP* violation in decay, resulting when the magnitudes of the amplitudes for a decay and for the *CP*-conjugate decay are different. In SM, the only weak phase besides the mixing phase is the phase of the CKM matrix. In SUSY-mediated processes new phases arise as well as new contributions to $B^0\bar{B}^0$ mixing. Experimentally, *CP* violation is present when an asymmetry between a process and its *CP* conjugate is observed. At the $\Upsilon(4S)$ the two B mesons are produced in opposite *CP* eigenstates. For such systems time-integrated *CP* asymmetries of B^0 and $\bar{B}^0$ mesons decaying into a *CP* eigenstate or into *CP*-conjugate states vanish. To observe an effect, one needs to measure the *CP* asymmetry as a function of the time difference Δt between the two B decays. Measurements of such time-dependent *CP* asymmetries provide a determination of the angles α, β and γ in the Unitarity Triangle [130]. For measurements of γ also other methods exist. The focus here is on measurements accessible in neutral and charged B decays.

The time-dependent *CP* asymmetry for a B decay into a *CP* eigenstate, f_{CP}, is defined by

$$\mathcal{A}_{CP}(\Delta t) = \frac{\Gamma(B^0 \to f_{CP})(\Delta t) - \Gamma(\bar{B}^0 \to f_{CP})(\Delta t)}{\Gamma(B^0 \to f_{CP})(\Delta t) + \Gamma(\bar{B}^0 \to f_{CP})(\Delta t)} = C_f \cos(\Delta m_{B_d}\Delta t) + S_f \sin(\Delta m_{B_d}\Delta t), \qquad (22)$$

where

$$C_f = \frac{(1- \mid \lambda \mid^2)}{(1+ \mid \lambda \mid^2)}, \quad S_f = 2\frac{\mathcal{I}m\lambda}{(1+ \mid \lambda \mid^2)}, \quad \text{and} \quad \lambda = \eta_f \frac{q}{p}\frac{\bar{A}}{A}. \tag{23}$$

The factor η_f indicates the *CP* eigenvalue of f_{CP}, yielding $\eta_f = \pm 1$ for $CP(f_{CP}) = \pm 1$, q/p represents the $B^0\bar{B}^0$ mixing contribution and $\bar{A}/A$ is the amplitude ratio for $\bar{B}^0 \to f_{CP}$ and $B^0 \to f_{CP}$, respectively. *CP* is violated if $\mid \lambda \mid \neq 1$ or $\mathcal{I}m\lambda \neq 0$. Experimentally, the measurement of $\mathcal{A}_{CP}(\Delta t)$ involves three steps: (i) the reconstruction of *CP* eigenstates states such as $B \to J/\psi K^0_S$ or $B \to \pi^+\pi^-$, (ii) the tagging of the b flavor at production point using for example the charge of a lepton or a kaon observed in the other B meson, and (iii) the measurement of the time difference Δt of the two B-decay vertices. To account for time-resolution effects, the measured *CP* asymmetry is parameterized by the periodic function in equation 22 convoluted with a time-resolution function. To account for errors in the tagging procedure, the measured amplitudes C_f and S_f contain in addition a dilution factor $D = 1 - 2w$, where w represents the fraction of mistagged events.

For $B \to J/\psi K^0_S$ and related modes one expects $\mid \lambda \mid = 1$ in SM. Thus, the first term in equation 22 vanishes and *CP* asymmetries measure $D \cdot S_f$ with $S_f = \sin 2\beta$. Using a sample of 29.7 fb^{-1} BABAR was the first to observe *CP* violation in the $B^0\bar{B}^0$ system. The *CP* sample contained 803 events of which 640 events remained after tagging and vertexing. By analyzing *CP* asymmetries of $B^0(\bar{B}^0)$ decays into $J/\psi K^0_S$, $\psi(2S)K^0_S$, $\chi_c K^0_S$, and $J/\psi K^0_L$, *CP* eigenstates as well as $J/\psi K^{*0}$ *CP* conjugate states, BABAR measured $\sin 2\beta = 0.59 \pm 0.14_{(stat)} \pm 0.05_{(sys)}$ [131]. BELLE confirmed the presence of *CP* violation measuring $\sin 2\beta = 0.99 \pm 0.14_{(stat)} \pm 0.06_{(sys)}$ [132]. The present world average of $\sin 2\beta = 0.79 \pm 0.1$ is consistent with a value of β obtained from measurements of the three sides of the Unitarity Triangle. However, presently the errors are rather large, mainly because of large theoretical uncertainties in the extraction of CKM parameters from measurements of semileptonic branching fractions, ϵ_k (parameterizing *CP* violation in $K^0\bar{K}^0$ mixing), and Δm_{B_d}. The measurement of α is complicated by contributions from penguin processes. Thus, both time-dependent terms in equation 22 are present and $\mathcal{I}m\lambda = \sin 2\alpha_{eff}$, where α and α_{eff} differ by a penguin phase δ_P. Furthermore, α-sensitive modes are $b \to u$ transitions that are suppressed with respect to $b \to c$ transitions by $\mid V_{ub}/V_{cb} \mid^2 = \mathcal{O}(10^{-2})$, thus requiring larger B samples than for $b \to c$ processes. So far α has not been measured directly. In a sample of 30.4 fb^{-1} BABAR has studied the time dependence of 65 $\pi^+\pi^-$ events, yielding $S_{\pi\pi} = 0.03^{+0.53}_{-0.56\ (stat)} \pm 0.11_{(sys)}$ and $C_{\pi\pi} = -0.25^{+0.45}_{-0.47\ (stat)} \pm 0.14_{(sys)}$ [133].

The measurements of the three angles in the Unitarity Triangle allow various tests. First, one checks for consistency between β measured directly in *CP* asymmetries and β obtained from measurements of the sides of the Unitarity Triangle. Second, one compares $\sin 2\beta$ measurements obtained in different quark processes, such as $b \to c\bar{c}s$, $b \to c\bar{c}d$ and $b \to s\bar{s}s$. In SM, all measurements have to give the same result. SUSY contributions, however, may affect each quark process differently. Thus, it is necessary to measure $\sin 2\beta$ also in $b \to c\bar{c}d$ processes such as $B \to D^{(*)+}D^{(*)-}$ or $B \to J/\psi\pi^0$ and in $b \to s\bar{s}s$ processes such as $B \to \phi K^0_S$ equally well as in $B \to J/\psi K^0_S$. Third, with the additional measurements of α the Unitarity Triangle is two-fold overconstrained. Fourth, *CP* asymmetries measured in $B \to J/\psi K^0_S$ and $B \to \pi^+\pi^-$, combined with measurement of the $B^0\bar{B}^0$ oscillation frequency Δm_{B_d} and that of $\mid V_{ub}/V_{cb} \mid$ allow a model-independent analysis to look for New Physics contributions. These can be parameterized in terms of a scale parameter $r_d = \Delta m^{exp}_{B_d}/\Delta m^{SM}_{B_d}$, that accounts for new contributions to $B^0\bar{B}^0$ mixing, and a new weak phase θ_d that represents new sources of *CP* violation [134, 135, 136]. Finally, with the measurement of γ one can test for closure of the Unitarity Triangle: $\alpha + \beta + \gamma = \pi$ [136].

In order to carry out these tests and to uncover SUSY contributions in *CP* asymmetries high-precision measurements are important. The present statistical uncertainty of $\sin 2\beta$ in BABAR is 0.14 for 29.7 fb^{-1}. The precision is expected to improve as $1/\sqrt{\mathcal{L}}$. Assuming that the reconstruction efficiency and tagging performance remain unchanged extrapolations to 100 fb^{-1} and 1 ab^{-1} yield statistical errors of $\sigma_{\sin 2\beta} = 0.076$ and $\sigma_{\sin 2\beta} = 0.024$, respectively. Since BELLE should achieve similar precisions, the error in the world average of $\sin 2\beta$ is reduced by another factor of $\sqrt{2}$. Contributions of the systematic error consists of tagging uncertainties, vertexing resolution, B life-time precision and background treatment. With increased statistics, the individual systematic errors will be reduced, so that the total systematic uncertainty should remain of the order of the statistical error. For an annual luminosity of 10 ab^{-1} at a super B factory the statistical error will be reduced to $\sigma_{\sin 2\beta} = 0.0076$. This should be compared with expectations at the LHC. Based on Monte Carlo simulations the statistical precision of $\sin 2\beta$ measured in *CP* asymmetries of $B \to J/\psi K^0_s$ is estimated to be $\sigma_{\sin 2\beta}(\psi K_s) = 0.017$ for ATLAS, $\sigma_{\sin 2\beta}(\psi K_s) = 0.015$ for CMS and $\sigma_{\sin 2\beta}(\psi K_s) = 0.021$ for LHCb for one year of LHC running [119]. In a sample of $2fb^{-1}$ at the Tevatron [118] precisions expected for $\sin 2\beta$ are $\sigma_{\sin 2\beta}(\psi K_s) = 0.05$ for CDF, $\sigma_{\sin 2\beta}(\psi K_s) = 0.04$ for D0, and $\sigma_{\sin 2\beta}(\psi K_s) = 0.025$ for BTEV. In the next 5-10 years, when the high luminosities will be achieved, the measurements of the sides of the Unitarity Triangle will also improve. Particularly, the theoretical uncertainties associated with the side measurements are expected to improve by a factor of 2-4 [109].

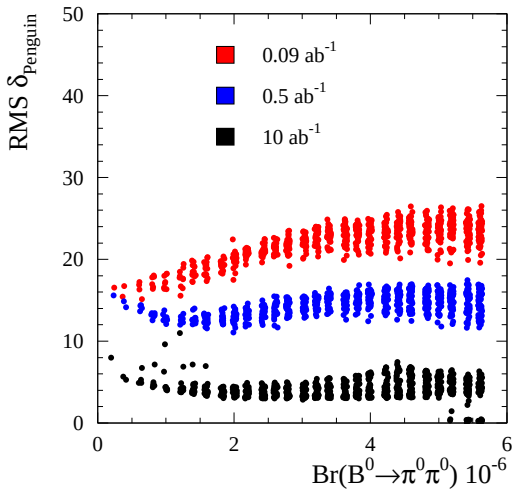

FIG. 8: Uncertainty in extracting the angle $\delta_P = \alpha_{eff} - \alpha$ in degrees versus the $B^0 \to \pi^0\pi^0$ branching fraction for samples of 90 fb^{-1}, 500 fb^{-1}, and 10 ab^{-1}.

For a comparison of $\sin 2\beta$ measurements in different quark processes precisions expected for $b \to s\bar{s}s$ and $b \to c\bar{c}d$ processes are not sufficient in present asymmetric B factories. In a sample of 22 fb^{-1} BABAR observes 11 $B \to \phi K^0_S$ events [137, 138]. Using the results of the BABAR $\sin 2\beta$ measurement and the observed ϕK^0_S yield gives statistical-error estimates of $\sigma_{\sin 2\beta}(\phi K_s) = 0.56$ for 100 fb^{-1}, $\sigma_{\sin 2\beta}(\phi K_s) = 0.18$ for 1 ab^{-1}, and $\sigma_{\sin 2\beta}(\phi K_s) = 0.056$ for 10 ab^{-1}. At these levels of precision systematic errors are less important. In the modes $B \to J/\psi\pi^0$ BABAR observes 13 events in a sample of 23 fb^{-1} [109]. Following the same extrapolation procedure as for ϕK^0_S the precision expected for $\sin 2\beta$ measurements in $J/\psi\pi^0$ is $\sigma_{\sin 2\beta}(J/\psi\pi^0) = 0.52$ in 100 fb^{-1}, $\sigma_{\sin 2\beta}(J/\psi\pi^0) = 0.16$ in 1 ab^{-1} and $\sigma_{\sin 2\beta}(J/\psi\pi^0) = 0.052$ in 10 ab^{-1}.

Measurements of $\sin 2\alpha$ also require high statistics, since branching fractions for $b \to u$ processes are small and are affected by competing penguin amplitudes. Extrapolating the present BABAR $B \to \pi^+\pi^-$ results to high luminosities yields $\sigma_{C_{\pi\pi}} = 0.26$, $\sigma_{S_{\pi\pi}} = 0.32$ for 100 fb^{-1}, $\sigma_{C_{\pi\pi}} = 0.09$, $\sigma_{S_{\pi\pi}} = 0.1$ for 1 ab^{-1}, and $\sigma_{C_{\pi\pi}} = 0.026$, $\sigma_{S_{\pi\pi}} = 0.032$ for 10 ab^{-1}. To extract α from $S_{\pi\pi}$ one needs to measure the penguin phase δ_P. This is achieved by exploiting isospin relations among the amplitudes of $B \to \pi\pi$ and $\bar{B} \to \pi\pi$ decays [139]. In the absence of electroweak-penguin amplitudes the isospin relations form two triangles (one for B and one for $\bar{B}$ decays) with a common amplitude base $A(B^+ \to \pi^+\pi^0) = A(B^- \to \pi^-\pi^0)$. The angle between the two triangles is $2\delta_P$. The presence of electroweak-penguin amplitudes introduces a small correction. The real challenge in this analysis, however, is the measurement of $\mathcal{B}(B^0 \to \pi^0\pi^0)$ and $\mathcal{B}(\bar{B}^0 \to \pi^0\pi^0)$, since branching fractions are rather small and the $\pi^0\pi^0$ final state is affected by a large $q\bar{q}$-continuum background. The determination of δ_P as a function of $\mathcal{B}(B^0 \to \pi^0\pi^0)$ is depicted in Figure 8 for three different luminosities. In a 10 ab^{-1} sample the uncertainty expected for δ_P is $\sigma_{\delta_P} = 5^o$, which is about a factor of three larger than the uncertainty expected for α_{eff} from $S_{\pi\pi}$. For 2 fb^{-1} BTEV estimates a statistical error of $\sqrt{\sigma^2_{C_{\pi\pi}} + \sigma^2_{S_{\pi\pi}}} = 0.024$ [118]. For comparison, LHCb quotes errors of $\sigma_{S_{\pi\pi}} = 0.07$ and $\sigma_{C_{\pi\pi}} = 0.09$ per year of LHC running. Using a Dalitz plot analysis in the $B \to \rho\pi$ channel is another promising method to extract α with high precision both at a super B factory and in future experiments at hadron machines. For example, LHCb quotes an expected statistical error of $\sigma_\alpha(\rho\pi) = 3 - 5^o$ per year of LHC running [119].

One promising method of measuring γ at the $\Upsilon(4S)$ is based on studying $B \to D^{(*)}K^{(*)}$ decays [140]. Here the different CKM structure in $b \to c\bar{u}s$ and $b \to u\bar{c}s$ processes is exploited, since the former decay has no weak phase while the latter involves γ. For the extraction of γ at least two D^0 flavor eigenstates, ($K^-\pi^+$, $K^-\pi^+\pi^0$, or $K^-\pi^+\pi^+\pi^-$) need to be reconstructed, since besides γ the $B^- \to \bar{D}^{(*)0}K^{(*)-}$ branching fraction and two strong phases need to be measured. Note, that this procedure leads to an eightfold ambiguity in the value of γ. To gain sufficient statistics actually all possible DK, D^*K, DK^* and D^*K^* modes have to be combined. In a sample of 600 fb^{-1} the statistical uncertainty in γ is estimated to range around $\sigma_\gamma \sim 5 - 10^o$ depending on the exact value of γ. Thus, for a range of two-three standard deviations each solution covers most of the γ region. In a sample of 10 ab^{-1}, however, this is different, as the statistical uncertainty is expected to be reduced to $\sigma_\gamma \sim 1 - 2.5^o$. So, again high-statistics B samples are required. In 2 fb^{-1} BTEV expects to measure γ with an error of about 7^o, using $B^0_s \to D^-_s K^+$ decays [118].

Another method of measuring γ in B decays involves CP asymmetries in $D^{(*)}\pi$ or $D^{(*)}\rho$ modes [141, 142, 143].

Here, the combination of CKM angles $2\beta+\gamma$ is measured, which results from an interference between the decay $b \to c\bar{u}d$ and the $B^0\bar{B}^0$-mixed process $\bar{b} \to \bar{u}c\bar{d}$, where the latter depends on the angle γ. BABAR recently studied the $D^{*+}\pi^-$ mode [109], which has a large branching fraction and can be partially reconstructed with low backgrounds but yields a small *CP* asymmetry. The main disadvantage of this technique is the necessity of measuring the ratio r of the doubly CKM-suppressed decay $\bar{b} \to \bar{u}c\bar{d}$ to the allowed decay $b \to c\bar{u}d$. Extrapolating the BABAR study yields statistical-error estimates of $\sigma_{\sin(2\beta+\gamma)}(D^*\pi) \sim 0.3$ for 100 fb^{-1}, $\sigma_{\sin(2\beta+\gamma)}(D^*\pi) \sim 0.1$ for 1 ab^{-1}, and $\sigma_{\sin(2\beta+\gamma)}(D^*\pi) \sim 0.03$ for 10 ab^{-1}. The probability that r is not measured due to statistical fluctuations is 30%, 10% and 3%, respectively. For comparison, LHCb expects to achieve a statistical error of $\sigma_{sin(2\beta+\gamma)} = 0.26$ per year of LHC running.

CP asymmetries of rare decays into flavor eigenstates are also rather suited to search for SUSY-mediated processes. For example in $B \to X_s\gamma$ decays *CP* asymmetries are expected to be small in SM ($\leq 1\%$) [144] but they may be enhanced up to 20% in SUSY models [145]. So far all observed *CP* asymmetries are consistent with zero. In the inclusive $B \to X_s\gamma$ mode CLEO measured $\mathcal{A}_{CP}(B \to X_s\gamma) = (-0.079 \pm 0.108 \pm 0.022) \times (1.0 \pm 0.03)$ [146], where the first error is statistical while the second and third errors represent additive and multiplicative systematic uncertainties, respectively. Though the *CP* asymmetry has been corrected for contributions from $B \to X_d$, a separation of these events from $B \to X_s\gamma$ events may become necessary on an event-by-event basis to rule out that the *CP* asymmetry in $B \to X_s\gamma$ is canceled by that in $B \to X_d\gamma$. In the exclusive $B^0 \to K^{*0}\gamma$ modes BABAR observed a *CP* asymmetry of $\mathcal{A}_{CP}(B \to K^{*0}\gamma) = -0.035 \pm 0.076 \pm 0.012$ using the three K^* final states, $K^+\pi^-$, $K^+\pi^0$ and $K^0_S\pi^+$ [117]. Extrapolating the measured statistical error to high luminosities yields $\sigma_{\mathcal{A}_{CP}} = 3.3\%$ (3.5%) for 100 fb^{-1}, $\sigma_{\mathcal{A}_{CP}} = 1.0\%$ (1.1%) for 1 ab^{-1} and $\sigma_{\mathcal{A}_{CP}} = 0.33\%$ (0.35%) for 10 ab^{-1} in $B \to X_s\gamma$ ($B \to K^*\gamma$) modes. LHCb expects to measure $\mathcal{A}_{CP}(B \to K^*\gamma)$ with a precision of 1% per year of running.

C. B Decays into Two Charged Leptons

Another interesting probe of supersymmetry is the decay $B_s \to \mu^+\mu^-$. The SM prediction is given by $\mathcal{B}(B_s \to \mu^+\mu^-) = (3.7 \pm 1.2) \times 10^{-9}$, with the uncertainty ($\pm 25\%$) dominated by the decay constant f_{B_s}. The current experimental bound on the branching ratio, ($\mathcal{B}$), has been set during Run-I of the Tevatron, where CDF [147] determined $\mathcal{B}(B_s \to \mu^+\mu^-) < 2.6 \times 10^{-6}$ at 90% C.L. In addition to the experimental challenge, the almost three orders of magnitude gap between the current experimental bound and the SM prediction makes this mode an excellent laboratory for new physics. In contrast to observables which enter the unitarity triangle [148], in the MSSM, the branching ratio $\mathcal{B}(B_s \to \mu^+\mu^-)$ grows like $\tan^6\beta$ [149, 150, 151, 152, 153], with a possible several orders of magnitude enhancement. More interestingly, it has been very recently shown [154] that in the mSUGRA scenario there is a strong correlation with the muon anomalous magnetic moment $(g-2)_\mu$. An interpretation of the recently measured excess in $(g-2)_\mu$ in terms of mSUGRA corrections implies a substantial supersymmetric enhancement of the branching ratio $\mathcal{B}(B_s \to \mu^+\mu^-)$: if $(g-2)_\mu$ exceeds the Standard Model prediction by $(\delta a_\mu)_{SUSY} = 4 \times 10^{-9}$, $\mathcal{B}(B_s \to \mu^+\mu^-)$ is larger by a factor of 10–100 than in the Standard Model and within reach of Run-II of the Tevatron. The single event sensitivity of CDF at Run-IIa is estimated to be 1.0×10^{-8}, for an integrated luminosity of 2 fb^{-1} [155]. Thus if mSUGRA corrections enhance $\mathcal{B}(B_s \to \mu^+\mu^-)$ to e.g. 5×10^{-7}, one will see 50 events in Run-IIa. Run-IIb may collect 10-20 fb^{-1} of integrated luminosity, which implies 250-500 events in this example.

Following Ref. [154], in Fig.9 we show the contours of $\mathcal{B}(B_s \to \mu^+\mu^-)$ (solid) and $(\delta a_\mu)_{SUSY}$ (dashed) in this plane, for $\tan\beta = 50$, $A_0 = 0$, $\mu > 0$ and $m_t = 175\,\text{GeV}$. The shaded region is excluded through the various theoretical and experimental constraints. A sensitivity of $\mathcal{B}(B_s \to \mu^+\mu^-) \sim 2 \times 10^{-7}$ at CDF now corresponds to a sensitivity of $M_{1/2} \sim 280\,\text{GeV}$ and $M_0 \sim 400\,\text{GeV}$, respectively. While CDF is not able to see squark masses directly up to 0.7 TeV (corresponding to $M_{1/2} = M_0 \simeq 300$ GeV), it will nevertheless be able to prepare the ground for LHC by observing the $B_s \to \mu^+\mu^-$ mode. Even better, after $10\,\text{fb}^{-1}$ CDF will probe $M_{1/2} \sim 450\,\text{GeV}$ and $M_0 \sim 600\,\text{GeV}$ (for $\tan\beta = 50$) which in mSUGRA corresponds to masses for the heaviest superpartners of 1 TeV. We conclude the discussion of Fig.9 with the prediction of the light Higgs boson mass M_h (dot-dashed line) for $\tan\beta = 50$ in the mSUGRA scenario [156]. Any measurement of $\mathcal{B}(B_s \to \mu^+\mu^-)$ by itself implies a useful *upper* bound on M_h. The simultaneous information of $\mathcal{B}(B_s \to \mu^+\mu^-)$ and δa_μ fixes M_h in most regions of the $(M_{1/2}, M_0)$-plane. A Higgs mass around 115.6 GeV results in $10^{-8} \sim \mathcal{B}(B_s \to \mu^+\mu^-) \sim 3 \times 10^{-7}$ which would most likely be measured before the Higgs boson is discovered.

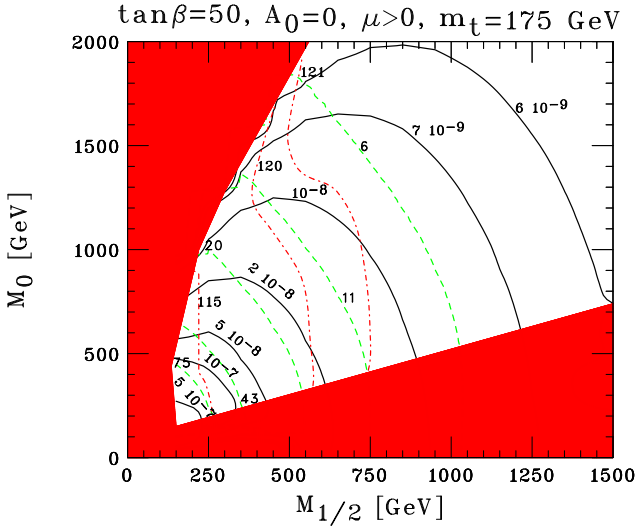

FIG. 9: Contour plots of the $\mathcal{B}(B_s \to \mu^+\mu^-)$ (solid) and on $(\delta a_\mu)_{SUSY}$ (dashed) in the $(M_0, M_{1/2})$-plane for mSUGRA parameter values as shown. Contours of the light Higgs boson mass (dot-dash line) are also shown. From Ref. [154].

VI. DIRECT DARK MATTER SEARCHES

Neutralinos in supersymmetry are well-motivated candidates to provide much or all of the non-baryonic dark matter. In many models, the neutralino is the LSP and is effectively stable. In general, the lightest neutralino is a mixture of the superpartners of Higgs and electroweak gauge bosons. Remarkably, detailed calculations of the thermal relic density of neutralinos have shown that neutralinos may indeed account for most of the missing mass of the universe.

Typically, there can be several different cosmologically preferred regions in parameter space. For example, in minimal supergravity, there are four: a 'bulk' region at relatively low m_0 and $m_{1/2}$, a 'focus-point' region [157, 158, 159] at relatively large m_0, a co-annihilation 'tail' extending out to relatively large $m_{1/2}$ [160, 161, 162], and a possible 'funnel' between the focus-point and co-annihilation regions due to rapid annihilation via direct-channel Higgs boson poles [163, 164]. A set of benchmark supersymmetric model parameter choices was proposed [165] just prior to Snowmass 2001, with points representing each of those regions. In this and the next section, we shall use this set of benchmarks to illustrate our discussion of the various signals of supersymmetric dark matter [166].

Neutralinos are very weakly interacting and they pass through collider detectors without leaving a trace. Therefore, it is practically impossible to observe them in collider experiments directly. Existing bounds on neutralinos must rely on model-dependent correlations between their properties and those of other supersymmetric particles. However, if neutralinos make up a significant portion of the halo dark matter, many additional avenues for their detection open up. They may deposit energy as they scatter off nuclei in terrestrial, usually sub-terrestrial, detectors.

Searches for this signal in low background detectors have been underway for around 20 years. The first decade was dominated by conventional HPGe (and Si) semiconductor detectors. The design of these detectors was to some extent "off-the-shelf" and progress was achieved, for the most part, by improving the radioactive backgrounds around the detectors. In the mid-90's results from NaI scintillator detectors became competitive. They were able to employ pulse shape discrimination to make statistical distinctions between populations of electron recoil events, and nuclear recoil events. In principle, the intrinsic background of the detector and environment were no longer the limiting factors, since with sufficient exposure time and target mass the limits could be driven down. However, the relatively poor quality of the NaI discrimination meant that systematic effects rapidly dominate, halting any further improvement with exposure. The NaI detector technology could also be described as off-the-shelf, however, the low background and high light yield housing systems were very definitely novel. At the end of 90's we finally saw results, from new cryogenic (<1 K) detector technology that had been developed specifically for direct detection, take the lead in terms of sensitivity.

Current sensitivities are now at a WIMP-nucleon normalized cross-section of 4×10^{-6} pb, which for a Ge target with a detection threshold of 10 keVr is an integrated event rate of 1.0 kg^{-1} d^{-1}. In this discussion keVr will be used to indicate actual recoil energy of an event, whereas keVee (electron equivalent), will be used to indicate the visible energy of a nuclear recoil event based on a energy scale for electron recoil events.

For example, in NaI scintillator, an iodine nuclear recoil of 22 keVr, generates the same light output as a 2 keVee electron event. To first approximation the differential recoil spectrum for WIMP nucleon events has a characteristic, but far from unique, exponential decay shape. This text is not the right place to discuss the details of what determines the spectrum, or the details of the cross-section normalization. See instead [167, 168].

We should touch on the DAMA experiment, which has reported a 4σ observation of annual modulation in the count rate of events in their lowest energy bins (2-6 keVee, which corresponds to 22-66 keVr for nuclear recoil events scattering on iodine) over a time spanning 4 years [169, 170]. The modulation has a phase (maximum in June) and a period (1 year) which would be consistent with the fluctuations in the observation arising from a contribution from a WIMP recoil spectrum which will be modulated by changes in the Earth's velocity in the galaxy. (Baseline model assumes an isothermal, non-co-rotating WIMP population.) It is enormously important that this signal be studied and the source clearly determined. The DAMA experiment will check its own results with two new years of data already available for analysis [171], and further data from running for the seventh year just beginning. It could be argued that a substantial overhaul in the data taking strategy should occur before further data taking, since the significance of the modulation effect is really systematics, rather than statistics limited, at this stage. The importance of a "beam-off" component of the data taking cannot be emphasized enough to establish the long term stability of data in the lowest energy bins when looking for few % fluctuation. While one cannot turn the WIMP wind off to order, a revised acquisition strategy that included direct calibration of the stability of the acceptance of the 2-3, 3-4, 4-5 keVee bins (in which all of the WIMP signal is expected) would help demonstrate that the modulation signal is not an artifact. Multiple scattering events should be stored, rather than vetoed since they could provide a non-WIMP calibration in real time. Additionally, on-line light pulses, or daily gamma calibrations, could be used to demonstrate the stability of the count rate in the bins if even higher statistics are required. The DAMA Collaboration is now constructing LIBRA, which will be a larger 250 kg array which by virtue of employing lower background NaI should be able to make a more sensitive check of the annual modulation signal. Using a different experimental setup will also help address the systematics question, although its operation at the same location, by the same collaboration doesn't allow all possible systematics to be checked. To this end the Boulby DM Collaboration may be able to carry through on the intention of running around 50 kg of NaI to cross-check the results directly with the same target material. Results from this Boulby program are unlikely to be available before 2004, however.

The currently reported results from the CDMS I [172] and EDELWEISS [173] experiments can be viewed as being inconsistent with the size of the annual modulation signal seen in DAMA. This is most readily seen by converting the published modulation amplitude of DAMA, into a cross-section on nucleon (1.4×10^{-5} pb), assuming scalar WIMP nucleon couplings, and then for comparison with CDMS I, to an estimated number of WIMP events (40) that would be observed in the 10.6 kg-live days exposure of Ge. This experiment saw 13 single scatter nuclear recoil events in Ge during this period which is clearly inconsistent with 40. In fact, the observation of an additional 4 multiple scattering nuclear recoil events during the same run, can be attributed unambiguously to neutrons. This permits a modest reduction of the (90% CL) upper limit in CDMS I single scatter nuclear recoil data to 8 WIMP events. On this basis, CDMS I and DAMA are inconsistent at 99.98%. The Edelweiss experiment has a similar WIMP sensitivity using detectors that are like the ones used in CDMS I. The data reported to date is for a smaller exposure of only 3 kg-days, however, it appears free of neutrons above a 25 keV analysis threshold due to the much deeper site location. Further data from longer exposure is eagerly awaited.

A number of avenues exist for reducing this incompatibility between the current results of the nuclear recoil discriminating Ge detectors and DAMA NaI annual modulation. Firstly, the DAMA collaboration reports an allowed region that combines not just the positive signal from the annual modulation amplitude, but also negative results/upper limits from other NaI derived data. This has the effect of reducing the headline expectation for the WIMP cross section by approximately a factor 3. This makes the disagreement between the experiments not statistically significant, but does beg the question whether the various DAMA experimental results themselves are mutually compatible. Alternative routes for explaining the apparently contradictory results have looked at the nature of WIMPs themselves. Comparison of Na, I and Ge recoil rates requires the assumption of a model. As has been said before the primary analysis of the experimental data is developed assuming scalar, or spin independent interactions. The interaction rates of the spin independent process often dominates because of the enhancement by the coherent scattering across multiple nucleons. However, in the absence of spin independent couplings, the relative spin dependent couplings will be stronger for an NaI target, in which both elements are monoisotopic with odd proton spin, compared to Ge, which has only 1 odd neutron spin isotope, with an 8% abundance in the natural element. Existing indirect WIMP detection experiments, are able to (partially) test the spin dependent hypothesis, ruling out some, but not all possible solutions (see next section). Another entertaining model is to suggest that the WIMPs themselves inelastically scatter from nuclei (i.e. WIMPs require internal transition to scatter, between low energy non-degenerate states.) Tuning of the excitation energy can ensure that a heavier nuclei (such as I) may be able to scatter WIMPs at a significantly enhanced rate relative

to Ge [174].

If we now look forward at some of the predicted goals of a few experiments over the next decade, it is immediately apparent that the forecast rate of progress appears to be rapidly accelerating when compared to historical progress. The question is whether this is simply a "triumph of hope over expectation", or represents a genuinely improved rate of progress that stems from applying detector technologies (2-phase Xe, semiconductor and scintillator cryogenic detectors, naked HPGe) that were "birthed" with this specific application in mind. We believe that the optimism is justified. At present, there are a number of experiments under construction (or that will be shortly) that will test for WIMP interactions in the range 1.0 kg^{-1} d^{-1} - 0.01 kg^{-1} d^{-1}. The CDMS II, EDELWEISS II and CRESST II which all employ low energy threshold (< 10 keV), nuclear recoil discriminating, cryogenic detectors will be deploying ≈ 10 kg of target.

There is also significant interest in liquid Xe for WIMP detection. In principle, Xe is well placed, having a photon yield similar to that of NaI, while potentially being capable of creating a radioactively cleaner target (especially if 85Kr is removed during isotopic enrichment stage). Nuclear recoil versus gamma discrimination is also possible, either by pulse shape analysis, which gives a relatively weak separation, and using a simulatneous measurement of the photon and electron-ion charge yield in Xe which is a much stronger method of discrimination. The Rome group [169] achieved early operation of Xe deep underground. A new program has been started by a Japanese group in Kamioka [175]. There is a major effort on Xe by the Boulby DM Collaboration [176] which is constructing a series of liquid Xe experiments at Boulby mine in the UK. ZEPLIN I, now running at Boulby, is based on pulse shape discrimination. ZEPLIN II makes use of simultaneous collection of scintillation and charge to achieve factors of 10-100 improved sensitivity, and ZEPLIN III incorporates a high E-yield in the liquid to enhance the recoil signal. A new US group, XENON, has also recently been proposed, centered at Columbia that would also use high field operation of two phase liquid-gas Xe.

A prototype 1 m^3 low pressure gas (CS2) detector, DRIFT, has also just started low background operation at Boulby [177].

The GENIUS [178, 179] and MAJORANA experiments have proposed to improve limits in WIMP searches by significant reduction in radioactive background levels, and exploitation of active Ge self-shielding. Nuclear recoil discrimination is not available for low energy events in conventional HP Ge detectors. It is worth noting that if these experiments can reduce low energy backgrounds by a factor 3000 from current levels (as projected by GENIUS for the complete 14 m liquid nitrogen shield) the limiting background becomes events from electron scattering of pp solar neutrino flux.

In order to move beyond a sensitivity level of 2×10^{-9} pb targets of 100-1000 kg (equivalent Ge) with very good nuclear recoil discrimination (rejecting >99.99% of electron events) will be necessary. A limiting sensitivity for realistic detector arrays, based on existing cryogenic detectors (such as CryoArray [180]), or liquid Xe (such as ZEPLIN-MAX [181] will be at an event level of 1 event per 100 kg per 1 year which is equivalent to a WIMP-nucleon cross-section of 10^{-10} pb.

Fig. 10 shows the spin-independent cross-section for neutralino-proton scattering for the benchmark points of [165], using two different codes: `Neutdriver` [168] and `SSARD` [182]. (Experiments sensitive to spin-dependent scattering have inferior reach [166].) One finds reasonable agreement, with the largest differences arising for points D and K, where the cross-section is abnormally small due to cancellations [183, 184]. For any given $\tan\beta$, the cancellations occur only for a specific limited range in the neutralino mass. Unfortunately, points D and K fall exactly into this category.

Fig. 10 also shows the projected sensitivities for a number of experiments listed in the figure caption. It should be emphasized that the CDMS II experimental reach, based on a modest target mass of 5 kg of Ge, will test a significant subset of SUSY models, and comes close to testing 4 of the benchmarks I, B, E and L. These could be reached by the larger (100 kg)/lower background GENIUS detector. Benchmarks G, F, C, A and J can be reached by 1 tonne discriminating detectors, such as CryoArray, or ZEPLIN-MAX, discussed above. Some of the benchmarks within reach of the direct detection experiements will not be reached by accelerators in this decade, illustrating the complementary nature of direct detection results.

VII. INDIRECT DARK MATTER SEARCHES

Indirect dark matter signals arise from enhanced pair annihilation rates of dark matter particles trapped in the gravitational wells at the centers of astrophysical bodies. The different signals can be classified according to the nature of the emitted particles.

While most of the neutralino annihilation products are quickly absorbed, neutrinos may propagate for long distances and be detected near the Earth's surface through their charged-current conversion to muons. High-energy muons produced by neutrinos from the centers of the Sun and Earth are, therefore, prominent signals for indirect dark matter detection [189, 190, 191, 192, 193, 194, 195, 196].

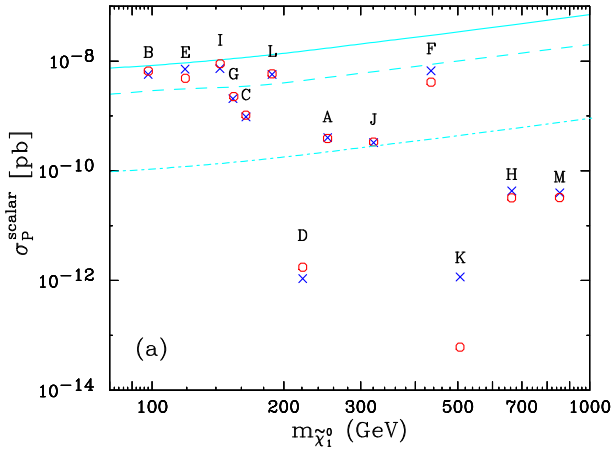

FIG. 10: *Elastic cross sections for spin-independent neutralino-proton scattering. The predictions of* `SSARD` *(blue crosses) and* `Neutdriver` *(red circles) are compared. Projected sensitivities for CDMS II [185] or CRESST [186] (solid); GENIUS [187] (dashed); CryoArray [180] or ZEPLIN-MAX [181] (dot-dashed) are also shown. (See Ref. [3].) Further theoretical and experimental direct detection data can be plotted using an interactive web plotter [188]. A cross section of* 4×10^{-6} *pb at a WIMP mass of 100 GeV (in line with current experimental sensitivities) would give an integrated event rate of 1.0 (1.2)* kg^{-1} d^{-1} *for a Ge (Xe) target with a detection threshold of 10 keVr. A cross section of* 10^{-10} *pb would give an integrated event rate of 1.0 (1.2)* $(100\ kg)^{-1}$ $year^{-1}$ *for Ge (Xe).*

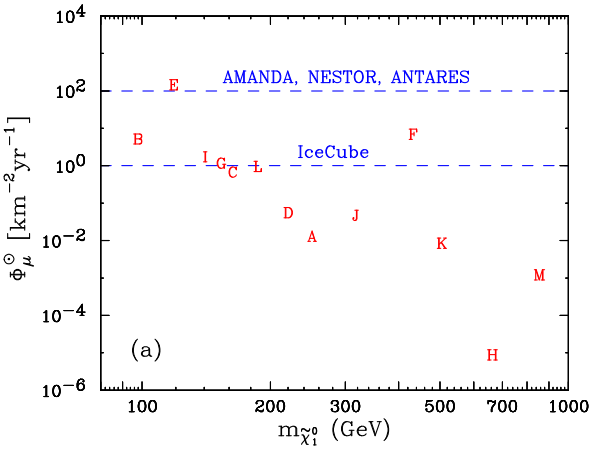

FIG. 11: *Muon fluxes from neutrinos originating from relic annihilations inside the Sun. Approximate sensitivities of near future neutrino telescopes (*$\Phi_\mu = 10^2$ km^{-2} yr^{-1} *for AMANDA II [197], NESTOR [198], and ANTARES [199], and* $\Phi_\mu = 1$ km^{-2} yr^{-1} *for IceCube [200]) are also indicated. (From Ref. [3].)*

Muon fluxes for each of the benchmark points are given in Fig. 11, using `Neutdriver` with a fixed constant local density $\rho_0 = 0.3$ GeV/cm^3 and neutralino velocity dispersion $\bar{v} = 270$ km/s (for further details, see [166]). For the points considered, rates from the Sun are far more promising than rates from the Earth [166, 195]. For the Sun, muon fluxes are for the most part anti-correlated with neutralino mass, with two strong exceptions: the focus point models (E and F) have anomalously large fluxes. In these cases, the dark matter's Higgsino content, though still small, is significant, leading to annihilations to gauge boson pairs, hard neutrinos, and enhanced detection rates.

The exact reach of neutrino telescopes depends on the salient features of the particular detector, *e.g.*, physical dimensions, muon energy threshold, etc., and the expected characteristics of the signal, *e.g.*, angular dispersion, energy spectrum and source (Sun or Earth). Two sensitivities, which are roughly indicative of the potential of upcoming neutrino telescope experiments, are given in Fig. 11. For focus point model E, where the neutralino is both light and significantly different from pure Bino-like, detection is possible already in the near future at AMANDA II [197], NESTOR [198], and ANTARES [199]. Point F may be within reach of IceCube [200], as the neutralino's significant Higgsino component compensates for its large mass. For point B, and possibly also points I, G, C, and L, the neutralino is nearly pure Bino, but is sufficiently light that detection at IceCube may also be possible.

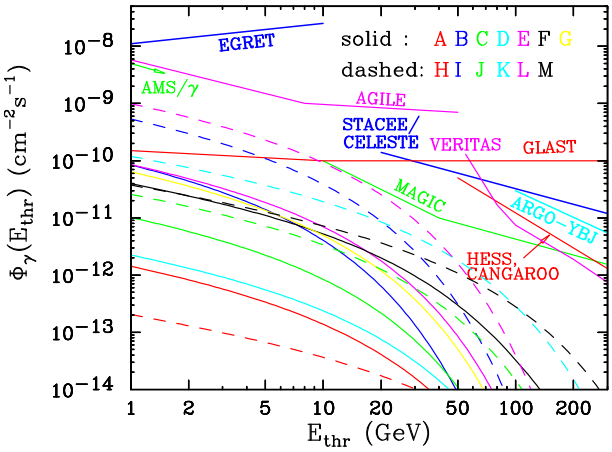

FIG. 12: *The integrated photon flux $\Phi_\gamma(E_{\rm th})$ as a function of photon energy threshold $E_{\rm th}$ for photons produced by relic annihilations in the galactic center. A moderate halo parameter $\bar{J} = 500$ is assumed [204]. Point source flux sensitivities for various gamma ray detectors are also shown. (From Ref. [3].)*

As with the centers of the Sun and Earth, the center of the galaxy may attract a significant overabundance of relic dark matter particles [201, 202, 203]. Relic pair annihilation at the galactic center will then produce an excess of photons, which may be observed in gamma ray detectors. While monoenergetic signals from $\chi\chi \to \gamma\gamma$ and $\chi\chi \to \gamma Z$ would be spectacular [204], they are loop-suppressed and rarely observable.

Fig. 12 shows the integrated photon flux $\Phi_\gamma(E_{\rm th})$ in the direction of the galactic center, computed following the procedure of [195]. Estimates for point source flux sensitivities of several gamma ray detectors, both current and planned, are also shown. The space-based detectors EGRET, AMS/γ and GLAST can detect soft photons, but are limited in flux sensitivity by their small effective areas. Ground-based telescopes, such as MAGIC, HESS, CANGAROO and VERITAS, are much larger and so sensitive to lower fluxes, but are limited by higher energy thresholds. These sensitivities are not strictly valid for observations of the galactic center. Nevertheless, they provide rough guidelines for what sensitivities may be expected in coming years. For a discussion of these estimates, their derivation, and references to the original literature, see [195].

Fig. 12 suggests that space-based detectors offer good prospects for detecting a photon signal, while ground-based telescopes have a relatively limited reach. GLAST appears to be particularly promising, with points I and L giving observable signals. One should keep in mind that all predicted fluxes scale linearly with $\bar{J}$, and for a different halo profiles may be enhanced or suppressed by up to two orders of magnitude. Such an enhancement may lead to detectable signals in GLAST for almost all points, and at MAGIC for the majority of benchmark points.

Relic neutralino annihilations in the galactic halo may also be detected through positron excesses in space-based and balloon experiments [205, 206, 207, 208]. Ref. [166] also estimated the observability of a positron excess, following the procedure advocated in [195]. For each benchmark spectrum, one first finds the positron energy $E_{\rm opt}$ at which the positron signal to background ratio S/B is maximized, and then requires S/B at $E_{\rm opt}$ to be within reach of the experiment. The sensitivities of a variety of experiments have been estimated in [195]. Among these experiments, the most promising is AMS [209], the anti-matter detector to be placed on the International Space Station. AMS will detect unprecedented numbers of positrons in a wide energy range. We estimate that a 1% excess in an fairly narrow energy bin, as is characteristic of the neutralino signal, will be statistically significant. Unfortunately, all benchmark points yield positron signals below the AMS sensitivity [166]. Similar rather pessimistic conclusions were derived in [210, 211]. Of course, one should be aware that as with the photon signal, positron rates are sensitive to the halo model assumed; for clumpy halos [212], the rate may be again enhanced by orders of magnitude [208].

Other possible indirect dark matter signals are antiprotons [193, 213, 214] and antideuterium [215], but those were not pursued during Snowmass 2001.

VIII. DISCUSSION AND CONCLUSIONS

Fig. 13 shows a compilation of many pre-LHC experiments in astrophysics, as well as particle physics at both the energy frontier and lower energies. The signals considered, the projected sensitivities, and the experiments likely to achieve them, are discussed in [4]. On the particle physics side, the signals considered were super-

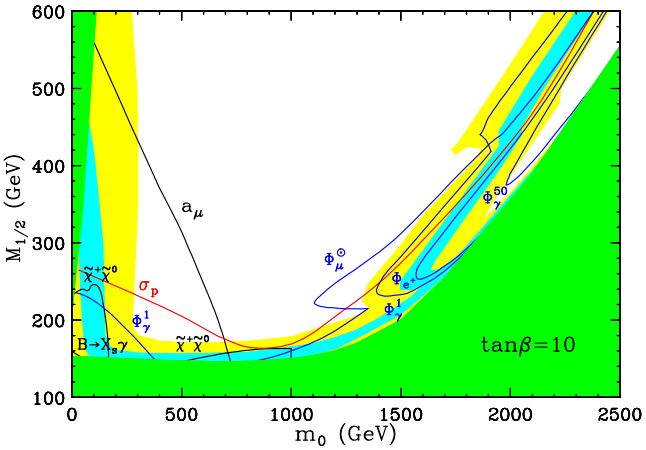

FIG. 13: Estimated reaches of various high-energy collider and low-energy precision searches, direct dark matter searches, and indirect dark matter searches before the LHC begins operation, for $\tan\beta = 10$. The projected sensitivities used are given in Ref. [4]. The darker shaded (green) regions are excluded by the requirement that the LSP be neutral (left) and by the LEP chargino mass limit (bottom and right). The regions with potentially interesting values of the LSP relic abundance: $0.025 \leq \Omega_\chi h^2 \leq 1$ (light-shaded, yellow) and $0.1 \leq \Omega_\chi h^2 \leq 0.3$ (medium-shaded, light blue), have also been delineated. The regions probed extend the curves toward the forbidden regions. (From Ref. [4].)

symmetry searches at LEP [216] and the Tevatron [217, 218, 219, 220, 221], the improved measurement of the $B \to X_s\gamma$ branching ratio at B-factories, as well as the projected final sensitivity of the Brookhaven $g_\mu - 2$ experiment. On the astrophysics side, the figure shows the projected reach of the upcoming direct dark matter detection experiments, as well as the multitude of other experiments to detect indirect neutrino, photon or positron signals from neutralino annihilations, as discussed earlier.

Several striking features emerge from Fig. 13. First, we see that, within the minimal supergravity framework, nearly all of the cosmologically preferred models will be probed by at least one experiment[2]. In the most natural regions, all models in which neutralinos form a significant fraction of dark matter will yield some signal before the LHC begins operation.

Also noteworthy is the complementarity of traditional particle physics searches and indirect dark matter searches. Collider searches require, of course, light superpartners. High precision probes at low energy also require light superpartners, as the virtual effects of superpartners quickly decouple as they become heavy. Thus, the LEP and Tevatron reaches are confined to the lower left-hand corner, as are, to a lesser extent, the searches for deviations in $B \to X_s\gamma$ and a_μ. These bounds, and all others of this type, are easily satisfied in the focus point models with large m_0, and indeed this is one of the virtues of these models. However, in the focus point models, *all* of the indirect searches are maximally sensitive, as the dark matter contains a significant Higgsino component. Direct dark matter probes share features with both traditional and indirect searches, and have sensitivity in both regions. It is only by combining all of these experiments, that the preferred region may be completely explored.

Finally, these results have implications for future colliders. In the cosmologically preferred regions of parameter space with $0.1 < \Omega_\chi h^2 < 0.3$, all models with charginos or sleptons lighter than 300 GeV will produce observable signals in at least one experiment. This is evident for $\tan\beta = 10$ in Fig. 13. In Fig. 14, we vary $\tan\beta$, fixing $M_{1/2}$ to 400 GeV, which roughly corresponds to 300 GeV charginos. We see that the preferred region is probed for any choice of $\tan\beta$. (For extremely low $\tan\beta$ and m_0, there appears to be a region that is not probed. However, this is excluded by current Higgs mass limits for $A_0 = 0$. These limits might be evaded if A_0 is also tuned to some extreme value, but in this case, top squark searches in Run II of the Tevatron [222] will provide an additional constraint.)

These results imply that if any superpartners are to be within reach of a 500 GeV lepton collider, some hint of supersymmetry must be seen before the LHC begins collecting data. This conclusion is independent of naturalness considerations. While our quantitative analysis is confined to minimal supergravity, we expect this result to be valid more generally. For moderate values of $\tan\beta$, if the dark matter is made up of neutralinos, they

[2] While this is strictly true for low $\tan\beta$, at higher $\tan\beta$ some of the preferred region may escape all probes, but this requires heavy superpartners and a significant fine-tuning of the electroweak scale [195]. Furthermore, the large $\tan\beta$ region is also effectively probed via the $B_s \to \mu^+\mu^-$ signal [154] which was not considered here.

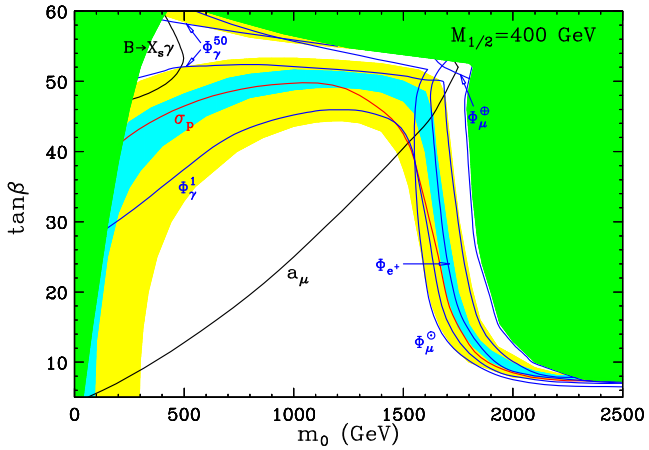

FIG. 14: As in Fig. 13, but in the $(m_0, \tan\beta)$ plane for fixed $M_{1/2} = 400$ GeV, $A_0 = 0$, and $\mu > 0$. The regions probed are toward the green regions, except for Φ_γ^{50}, where it is between the two contours. The top excluded region is forbidden by limits on the *CP*-odd Higgs scalar mass. (From Ref. [4].)

must either be light, Bino-like, or a gaugino-Higgsino mixture. If they are light, charginos will be discovered. If they are Bino-like, light sfermions are required to mediate their annihilation, and there will be anomalies in low energy precision measurements. And if they are a gaugino-Higgsino mixture, at least one indirect dark matter search will see a signal. For large $\tan\beta$, low energy probes become much more effective and again there is sensitivity to all superpartner spectra with light superpartners. Thus it appears, on qualitative grounds, that all models in which the scalar masses are not widely separated, and the charginos are not extravagantly heavy, will be accessible prior to LHC operation.

The most sensitive tests for SUSY contributions in B decays before the start of the LHC will come from $\sin 2\beta$ measurements in charmonium modes and *CP*-asymmetry measurements of $B \to X_s\gamma$ and $B \to K^*\gamma$ by BABAR and BELLE. For the latter studies the large SM theoretical uncertainties present in the branching-fraction measurements that make an extraction of SUSY contributions difficult are absent. In the LHC era improved measurements on $\sin 2\beta$ and the *CP* asymmetry in $K^{*0}\gamma$ will be carried out. In addition, measurements of branching-fractions and lepton forward-backward asymmetries of $B \to s\ell^+\ell^-$ modes will provide very sensitive tests for uncovering SUSY effects. While hadron-collider experiments will focus on $K^{(*)}\mu^+\mu^-$ modes, asymmetric B-factory experiments will study $B \to X_s\ell^+\ell^-$ and $B \to K^{(*)}\ell^+\ell^-$ decays. At a super B factory the precision can be significantly improved in these modes. While the first studies of α will be performed by BABAR and BELLE, precise measurements will come from from BTEV and LHCb. In particular, the hadron-collider experiments produce high statistics B_s samples, which allow for precise measurements of γ. Additional precise measurements of γ at the $\Upsilon(4S)$ can only come from a super B factory. By this time a considerable reduction of the theoretical uncertainties in the extraction of $|V_{ub}/V_{cb}|$, $|V_{td}|$ and $|V_{ts}|$ from data is also expected, allowing to perform a sensitive model-independent analysis for extracting a new weak phase and new contributions to $B^0\bar{B}^0$ mixing. In order to observe the modes $B \to X_s\nu\bar{\nu}$, $B \to K^+\nu\bar{\nu}$, or $B \to K^{*0}\nu\bar{\nu}$, which bear the least theoretical uncertainties of radiative penguin decays, and study their properties a super B factory is a prerequisite. So, for at least the next ten years a vivacious B physics program ensures many high-precision measurements of *CP* asymmetries and radiative penguin decay properties that are suitable for extracting SUSY contributions.

Acknowledgments

We thank E. A. Hinds, L. Littenberg, D. Miller and J. M. Pendlebury for sharing their wisdom.

[1] J. L. Feng, K. T. Matchev, and Y. Shadmi (2001), hep-ph/0110157.
[2] J. L. Feng and K. T. Matchev (2001), hep-ph/0111004.
[3] J. R. Ellis, J. L. Feng, A. Ferstl, K. T. Matchev, and K. A. Olive (2001), hep-ph/0111294.
[4] J. L. Feng, K. T. Matchev, and F. Wilczek (2001), hep-ph/0111295.

[5] G. Eigen, talk in P3-2 session, preprint P3-41, Proceedings of Snowmass Wokshop.
[6] G. Eigen, talk in E2 session, preprint E2-41, Proceedings of Snowmass Wokshop.
[7] H. N. Brown et al. (Muon g-2), Phys. Rev. Lett. **86**, 2227 (2001), hep-ex/0102017.
[8] M. Knecht and A. Nyffeler (2001), hep-ph/0111058.
[9] M. Knecht, A. Nyffeler, M. Perrottet, and E. De Rafael (2001), hep-ph/0111059.
[10] H. Masashi and T. Kinoshita (2001), hep-ph/0112102.
[11] I. Blokland, A. Czarnecki, and K. Melnikov (2001), hep-ph/0112117.
[12] J. Bijnens, E. Pallante, and J. Prades (2001), hep-ph/0112255.
[13] K. Melnikov, Int. J. Mod. Phys. **A16**, 4591 (2001), hep-ph/0105267.
[14] J. F. De Troconiz and F. J. Yndurain (2001), hep-ph/0106025.
[15] G. Cvetic, T. Lee, and I. Schmidt, Phys. Lett. **B520**, 222 (2001), hep-ph/0107069.
[16] A. Czarnecki and W. J. Marciano, Phys. Rev. **D64**, 013014 (2001), hep-ph/0102122.
[17] P. Fayet (1980), contributed to Europhysics Study Conf. on Unification of Fundamental Interactons, Erice, Italy, Mar 17-24, 1980.
[18] J. A. Grifols and A. Mendez, Phys. Rev. **D26**, 1809 (1982).
[19] J. R. Ellis, J. S. Hagelin, and D. V. Nanopoulos, Phys. Lett. **B116**, 283 (1982).
[20] R. Barbieri and L. Maiani, Phys. Lett. **B117**, 203 (1982).
[21] D. A. Kosower, L. M. Krauss, and N. Sakai, Phys. Lett. **B133**, 305 (1983).
[22] T. C. Yuan, R. Arnowitt, A. H. Chamseddine, and P. Nath, Zeit. Phys. **C26**, 407 (1984).
[23] T. Moroi, Phys. Rev. **D53**, 6565 (1996), hep-ph/9512396.
[24] M. Carena, G. F. Giudice, and C. E. M. Wagner, Phys. Lett. **B390**, 234 (1997), hep-ph/9610233.
[25] E. Gabrielli and U. Sarid, Phys. Rev. Lett. **79**, 4752 (1997), hep-ph/9707546.
[26] K. T. Mahanthappa and S. Oh, Phys. Rev. **D62**, 015012 (2000), hep-ph/9908531.
[27] J. L. Feng and K. T. Matchev, Phys. Rev. Lett. **86**, 3480 (2001), hep-ph/0102146.
[28] L. L. Everett, G. L. Kane, S. Rigolin, and L.-T. Wang, Phys. Rev. Lett. **86**, 3484 (2001), hep-ph/0102145.
[29] E. A. Baltz and P. Gondolo, Phys. Rev. Lett. **86**, 5004 (2001), hep-ph/0102147.
[30] U. Chattopadhyay and P. Nath, Phys. Rev. Lett. **86**, 5854 (2001), hep-ph/0102157.
[31] S. Komine, T. Moroi, and M. Yamaguchi, Phys. Lett. **B506**, 93 (2001), hep-ph/0102204.
[32] J. Hisano and K. Tobe, Phys. Lett. **B510**, 197 (2001), hep-ph/0102315.
[33] T. Ibrahim, U. Chattopadhyay, and P. Nath, Phys. Rev. **D64**, 016010 (2001), hep-ph/0102324.
[34] J. R. Ellis, D. V. Nanopoulos, and K. A. Olive, Phys. Lett. **B508**, 65 (2001), hep-ph/0102331.
[35] R. Arnowitt, B. Dutta, B. Hu, and Y. Santoso, Phys. Lett. **B505**, 177 (2001), hep-ph/0102344.
[36] K. Choi, K. Hwang, S. K. Kang, K. Y. Lee, and W. Y. Song, Phys. Rev. **D64**, 055001 (2001), hep-ph/0103048.
[37] J. E. Kim, B. Kyae, and H. M. Lee, Phys. Lett. **B520**, 298 (2001), hep-ph/0103054.
[38] S. P. Martin and J. D. Wells, Phys. Rev. **D64**, 035003 (2001), hep-ph/0103067.
[39] S. Komine, T. Moroi, and M. Yamaguchi, Phys. Lett. **B507**, 224 (2001), hep-ph/0103182.
[40] S.-w. Baek, P. Ko, and H. S. Lee (2001), hep-ph/0103218.
[41] D. F. Carvalho, J. R. Ellis, M. E. Gomez, and S. Lola, Phys. Lett. **B515**, 323 (2001), hep-ph/0103256.
[42] H. Baer, C. Balazs, J. Ferrandis, and X. Tata, Phys. Rev. **D64**, 035004 (2001), hep-ph/0103280.
[43] S.-w. Baek, T. Goto, Y. Okada, and K.-i. Okumura, Phys. Rev. **D64**, 095001 (2001), hep-ph/0104146.
[44] D. G. Cerdeno, E. Gabrielli, S. Khalil, C. Munoz, and E. Torrente-Lujan, Phys. Rev. **D64**, 093012 (2001), hep-ph/0104242.
[45] Z. Chacko and G. D. Kribs, Phys. Rev. **D64**, 075015 (2001), hep-ph/0104317.
[46] T. Blazek and S. F. King, Phys. Lett. **B518**, 109 (2001), hep-ph/0105005.
[47] G.-C. Cho and K. Hagiwara, Phys. Lett. **B514**, 123 (2001), hep-ph/0105037.
[48] R. Adhikari and G. Rajasekaran (2001), hep-ph/0107279.
[49] M. Byrne, C. Kolda, and J. E. Lennon (2001), hep-ph/0108122.
[50] S. Komine and M. Yamaguchi (2001), hep-ph/0110032.
[51] U. Chattopadhyay and P. Nath (2001), hep-ph/0110341.
[52] M. Endo and T. Moroi (2001), hep-ph/0110383.
[53] M. Graesser and S. Thomas (2001), hep-ph/0104254.
[54] A. Djouadi, M. Drees, and J. L. Kneur, JHEP **08**, 055 (2001), hep-ph/0107316.
[55] J. L. Feng and T. Moroi, Phys. Rev. **D61**, 095004 (2000), hep-ph/9907319.
[56] U. Chattopadhyay, D. K. Ghosh, and S. Roy, Phys. Rev. **D62**, 115001 (2000), hep-ph/0006049.
[57] A. D. Sakharov, Pisma Zh. Eksp. Teor. Fiz. **5**, 32 (1967).
[58] G. R. Farrar and M. E. Shaposhnikov, Phys. Rev. **D50**, 774 (1994), hep-ph/9305275.
[59] M. B. Gavela, P. Hernandez, J. Orloff, and O. Pene, Mod. Phys. Lett. **A9**, 795 (1994), hep-ph/9312215.
[60] M. B. Gavela, P. Hernandez, J. Orloff, O. Pene, and C. Quimbay, Nucl. Phys. **B430**, 382 (1994), hep-ph/9406289.
[61] P. Huet and E. Sather, Phys. Rev. **D51**, 379 (1995), hep-ph/9404302.
[62] F. Hoogeveen, Nucl. Phys. **B341**, 322 (1990).
[63] I. B. Khriplovich, Phys. Lett. **B173**, 193 (1986).
[64] E. D. Commins, S. B. Ross, D. DeMille, and B. C. Regan, Phys. Rev. **A50**, 2960 (1994).
[65] E. Hinds (2001), talk given at 'KAON 2001', Pisa, June 12-17, 2001.
[66] E. Hinds, informal communication.
[67] J. M. Pendlebury and E. A. Hinds, Nucl. Instrum. Meth. **A440**, 471 (2000).

[68] P. G. Harris et al., Phys. Rev. Lett. **82**, 904 (1999).
[69] M. V. Romalis, W. C. Griffith, and E. N. Fortson, Phys. Rev. Lett. **86**, 2505 (2001), hep-ex/0012001.
[70] S. Dimopoulos and D. W. Sutter, Nucl. Phys. **B452**, 496 (1995), hep-ph/9504415.
[71] T. Ibrahim and P. Nath (2001), hep-ph/0107325.
[72] J. R. Ellis, S. Ferrara, and D. V. Nanopoulos, Phys. Lett. **B114**, 231 (1982).
[73] M. Dugan, B. Grinstein, and L. J. Hall, Nucl. Phys. **B255**, 413 (1985).
[74] A. G. Cohen, D. B. Kaplan, and A. E. Nelson, Phys. Lett. **B388**, 588 (1996), hep-ph/9607394.
[75] J. Bagger, J. L. Feng, and N. Polonsky, Nucl. Phys. **B563**, 3 (1999), hep-ph/9905292.
[76] J. A. Bagger, J. L. Feng, N. Polonsky, and R.-J. Zhang, Phys. Lett. **B473**, 264 (2000), hep-ph/9911255.
[77] J. L. Feng and K. T. Matchev, Phys. Rev. **D63**, 095003 (2001), hep-ph/0011356.
[78] K. S. Babu, B. Dutta, and R. N. Mohapatra, Phys. Rev. **D61**, 091701 (2000), hep-ph/9905464.
[79] T. Ibrahim and P. Nath, Phys. Rev. **D58**, 111301 (1998), hep-ph/9807501.
[80] M. Brhlik, G. J. Good, and G. L. Kane, Phys. Rev. **D59**, 115004 (1999), hep-ph/9810457.
[81] A. Manohar and H. Georgi, Nucl. Phys. **B234**, 189 (1984).
[82] M. Pospelov and A. Ritz, Phys. Rev. **D63**, 073015 (2001), hep-ph/0010037.
[83] T. Falk, K. A. Olive, M. Pospelov, and R. Roiban, Nucl. Phys. **B560**, 3 (1999), hep-ph/9904393.
[84] V. D. Barger et al., Phys. Rev. **D64**, 056007 (2001), hep-ph/0101106.
[85] Y. K. Semertzidis et al. (1999), hep-ph/0012087.
[86] J. Bailey et al. (CERN-Mainz-Daresbury), Nucl. Phys. **B150**, 1 (1979).
[87] J. Aysto et al. (2001), hep-ph/0109217.
[88] J. L. Feng, K. T. Matchev, and Y. Shadmi, Nucl. Phys. **B613**, 366 (2001), hep-ph/0107182.
[89] A. Romanino and A. Strumia (2001), hep-ph/0108275.
[90] T. Ibrahim and P. Nath, Phys. Rev. **D64**, 093002 (2001), hep-ph/0105025.
[91] J. S. Hagelin, S. Kelley, and T. Tanaka, Nucl. Phys. **B415**, 293 (1994).
[92] F. Gabbiani, E. Gabrielli, A. Masiero, and L. Silvestrini, Nucl. Phys. **B477**, 321 (1996), hep-ph/9604387.
[93] J. A. Bagger, K. T. Matchev, and R.-J. Zhang, Phys. Lett. **B412**, 77 (1997), hep-ph/9707225.
[94] M. L. Brooks et al. (MEGA), Phys. Rev. Lett. **83**, 1521 (1999), hep-ex/9905013.
[95] U. Bellgardt et al. (SINDRUM), Nucl. Phys. **B299**, 1 (1988).
[96] J. Kaulard et al. (SINDRUM II), Phys. Lett. **B422**, 334 (1998).
[97] T. Mori and *et al.* (1999), http://meg.psi.ch/doc/prop/index.html.
[98] M. Bachman and *et al.* (1997), http://meco.ps.uci.edu.
[99] R. Barbieri, L. J. Hall, and A. Strumia, Nucl. Phys. **B445**, 219 (1995), hep-ph/9501334.
[100] L. Randall and R. Sundrum, Nucl. Phys. **B557**, 79 (1999), hep-th/9810155.
[101] D. E. Kaplan, G. D. Kribs, and M. Schmaltz, Phys. Rev. **D62**, 035010 (2000), hep-ph/9911293.
[102] Z. Chacko, M. A. Luty, A. E. Nelson, and E. Ponton, JHEP **01**, 003 (2000), hep-ph/9911323.
[103] S. Ahmed et al. (CLEO), Phys. Rev. **D61**, 071101 (2000), hep-ex/9910060.
[104] M. Dine, Y. Grossman, and S. Thomas (2001), hep-ph/0111154.
[105] N. V. Krasnikov, Phys. Lett. **B388**, 783 (1996), hep-ph/9511464.
[106] N. Arkani-Hamed, H.-C. Cheng, J. L. Feng, and L. J. Hall, Phys. Rev. Lett. **77**, 1937 (1996), hep-ph/9603431.
[107] N. Arkani-Hamed, J. L. Feng, L. J. Hall, and H.-C. Cheng, Nucl. Phys. **B505**, 3 (1997), hep-ph/9704205.
[108] R. Ammar and *et al.* (CLEO collaboration), Phys. Rev. Lett. **70**, 138 (1993).
[109] P. Burchat and *et al.*, Physics at 10^{36}, Proceedings of Snowmass Wokshop.
[110] K. Chetyrkin, M. Misiak, and M. Munz, Phys. Lett. **B400**, 206 (1997).
[111] P. Gambino and M. Misiak, Nucl. Phys. **B611**, 338 (2001).
[112] S. Chen and *et al.* (CLEO collaboration), hep-ex/0108032.
[113] J. Hewett and J. Wells, Phys. Rev. **D55**, 5549 (1996).
[114] J. Hewett, Private communication.
[115] S. Bosch and G. Buchalla, hep-ph/0108081.
[116] M. Beneke, T. Feldmann, and D. Seidel, Nucl. Phys. **B612**, 25 (2001).
[117] A. Ryd and *et al.* (BABAR collaboration), Proc. of Int. Symp. on Heavy Flavor Physics 9.
[118] D. Atwood and *et al.*, Fermilab Pub 01/197.
[119] P. Ball and *et al.*, hep-ph/0003238.
[120] A. Ali, T. Mannel, and T. Morozumi, Phys. Lett. **B273**, 505 (1991).
[121] M. Misiak, Nucl. Phys. **B393**, 23 (1993).
[122] A. Buras and M. Munz, Phys. Rev. **D52**, 186 (1995).
[123] T. Coan and *et al.* (CLEO collaboration), Phys. Rev. Lett. **80**, 2289 (1997).
[124] D. Melikhov, N. Nikitin, and S. Simula, Phys. Lett. **B410**, 290 (1997).
[125] A. Ali and *et al.*, Phys. Rev. **D61**, 074024 (2000).
[126] K. Abe and *et al.* (BELLE collaboration), hep-ex/0109026.
[127] Y. Grossman, Z. Ligeti, and E. Nardi, Nucl. Phys. **B465**, 369 (1996).
[128] Y. Grossman, Z. Ligeti, and E. Nardi, Nucl. Phys. **B480**, 753 (1996).
[129] A. Ali, G. Giudice, and T. Mannel, Z. Phys. **C67**, 417 (1995).
[130] A. Buras and R. Fleischer, Adv. Ser. Direct. High Energy Phys. **15**, 65 (1998).
[131] B. Aubert and *et al.* (BABAR collaboration), Phys. Rev. Lett. **87**, 091801 (2001).
[132] K. Abe and *et al.* (BELLE collaboration), Phys. Rev. Lett. **87**, 091802 (2001).

[133] B. Aubert and *et al.* (BABAR collaboration), hep-ph/0107074.
[134] J. Soares and L. Wolfenstein, Phys. Rev. **D47**, 1021 (1995).
[135] Y. Grossman, Y. Nir, and M. Worah, Phys. Lett. **B407**, 307 (1997).
[136] D. Boutigny and *et al.* (BABAR collaboration), BABAR physics book, SLAC-PUB-504 (1998).
[137] B. Aubert and *et al.* (BABAR collaboration), hep-ph/0105001.
[138] R. Briere and *et al.* (CLEO collaboration), Phys. Rev. Lett. **86**, 3718 (2001).
[139] M. Gronau and D. London, Phys. Rev. Lett. **65**, 3381 (1990).
[140] D. Atwood, I. Dunietz, and A. Soni, Phys. Rev. Lett. **78**, 3257 (1997).
[141] I. Dunietz and R. G. Sachs, Phys. Rev. **D37**, 3186 (1988).
[142] R. Aleksan, I.Dunietz, and B. Kayser, Z. Phys. **C54**, 653 (1992).
[143] I.Dunietz, Phys. Lett. **B427**, 179 (1998).
[144] J. Soares, Nucl. Phys. **B367**, 575 (1991).
[145] A. Kagan and M. Neubert, Phys. Rev. **D58**, 094012 (1998).
[146] T. Coan and *et al.* (CLEO collaboration), Phys. Rev. Lett. **86**, 5661 (2001).
[147] F. Abe et al. (CDF), Phys. Rev. **D57**, 3811 (1998).
[148] A. Bartl et al., Phys. Rev. **D64**, 076009 (2001), hep-ph/0103324.
[149] K. S. Babu and C. Kolda, Phys. Rev. Lett. **84**, 228 (2000), hep-ph/9909476.
[150] C.-S. Huang, W. Liao, and Q.-S. Yan, Phys. Rev. **D59**, 011701 (1999), hep-ph/9803460.
[151] P. H. Chankowski and L. Slawianowska, Phys. Rev. **D63**, 054012 (2001), hep-ph/0008046.
[152] C. Bobeth, T. Ewerth, F. Kruger, and J. Urban, Phys. Rev. **D64**, 074014 (2001), hep-ph/0104284.
[153] G. Isidori and A. Retico, JHEP **11**, 001 (2001), hep-ph/0110121.
[154] A. Dedes, H. K. Dreiner, and U. Nierste (2001), hep-ph/0108037.
[155] D. Atwood and *et al.*, *B physics at the tevatron: Run-ii and beyond* (preliminary), fERMILAB-Pub-01/197.
[156] S. Ambrosanio, A. Dedes, S. Heinemeyer, S. Su, and G. Weiglein (2001), hep-ph/0106255.
[157] J. L. Feng, K. T. Matchev, and T. Moroi, Phys. Rev. Lett. **84**, 2322 (2000), hep-ph/9908309.
[158] J. L. Feng, K. T. Matchev, and T. Moroi, Phys. Rev. **D61**, 075005 (2000), hep-ph/9909334.
[159] J. L. Feng, K. T. Matchev, and F. Wilczek, Phys. Lett. **B482**, 388 (2000), hep-ph/0004043.
[160] J. R. Ellis, T. Falk, and K. A. Olive, Phys. Lett. **B444**, 367 (1998), hep-ph/9810360.
[161] J. R. Ellis, T. Falk, K. A. Olive, and M. Srednicki, Astropart. Phys. **13**, 181 (2000), hep-ph/9905481.
[162] M. E. Gomez, G. Lazarides, and C. Pallis, Phys. Rev. **D61**, 123512 (2000), hep-ph/9907261.
[163] J. R. Ellis, T. Falk, G. Ganis, K. A. Olive, and M. Srednicki, Phys. Lett. **B510**, 236 (2001), hep-ph/0102098.
[164] A. B. Lahanas and V. C. Spanos (2001), hep-ph/0106345.
[165] M. Battaglia et al. (2001), hep-ph/0106204.
[166] J. R. Ellis, J. L. Feng, A. Ferstl, K. T. Matchev, and K. A. Olive (2001), astro-ph/0110225.
[167] J. D. Lewin and P. F. Smith, Astropart. Phys. **6**, 87 (1996).
[168] G. Jungman, M. Kamionkowski, and K. Griest, Phys. Rept. **267**, 195 (1996), hep-ph/9506380.
[169] R. Bernabei et al., Phys. Lett. **B424**, 195 (1998).
[170] R. Bernabei et al., Nucl. Phys. Proc. Suppl. **91**, 361 (2001).
[171] P. Belli et al. (2001), hep-ph/0112018.
[172] R. Abusaidi et al. (CDMS), Nucl. Instrum. Meth. **A444**, 345 (2000), astro-ph/0002471.
[173] A. Benoit et al. (EDELWEISS), Phys. Lett. **B513**, 15 (2001), astro-ph/0106094.
[174] D. R. Smith and N. Weiner, Phys. Rev. **D64**, 043502 (2001), hep-ph/0101138.
[175] Y. Suzuki (Xenon) (2000), hep-ph/0008296.
[176] N. J. C. Spooner et al., p. 365 (2000), prepared for 4th International Symposium on Sources and Detection of Dark Matter in the Universe (DM 2000), Marina del Rey, California, 23-25 Feb 2000.
[177] C. J. Martoff, D. P. Snowden-Ifft, T. Ohnuki, N. Spooner, and M. Lehner, Nucl. Instrum. Meth. **A440**, 355 (2000).
[178] H. V. Klapdor-Kleingrothaus and B. Majorovits (2000), hep-ph/0103079.
[179] L. Baudis et al. (2000), hep-ex/0012022.
[180] R. J. Gaitskell (2001), astro-ph/0106200.
[181] N. J. C. Spooner and V. A. Kudryavtsev (2001), astro-ph/0111053.
[182] T. Falk, G. Ganis, J. McDonald, K. A. Olive, and M. Srednicki, unpublished.
[183] J. R. Ellis, A. Ferstl, and K. A. Olive, Phys. Lett. **B481**, 304 (2000), hep-ph/0001005.
[184] J. R. Ellis, A. Ferstl, and K. A. Olive (2001), hep-ph/0111064.
[185] R. W. Schnee et al., Phys. Rept. **307**, 283 (1998).
[186] M. Bravin et al. (CRESST-Collaboration), Astropart. Phys. **12**, 107 (1999), hep-ex/9904005.
[187] H. V. Klapdor-Kleingrothaus (2000), hep-ph/0104028.
[188] R. Gaitskell and V. Mandic, interactive data plotter maintained at http://dmtools.berkeley.edu.
[189] J. Silk, K. A. Olive, and M. Srednicki, Phys. Rev. Lett. **55**, 257 (1985).
[190] K. Freese, Phys. Lett. **B167**, 295 (1986).
[191] L. M. Krauss, M. Srednicki, and F. Wilczek, Phys. Rev. **D33**, 2079 (1986).
[192] L. Bergstrom, J. Edsjo, and P. Gondolo, Phys. Rev. **D58**, 103519 (1998), hep-ph/9806293.
[193] A. Bottino, F. Donato, N. Fornengo, and S. Scopel, Astropart. Phys. **10**, 203 (1999), hep-ph/9809239.
[194] A. Corsetti and P. Nath, Int. J. Mod. Phys. **A15**, 905 (2000), hep-ph/9904497.
[195] J. L. Feng, K. T. Matchev, and F. Wilczek, Phys. Rev. **D63**, 045024 (2001), astro-ph/0008115.
[196] V. D. Barger, F. Halzen, D. Hooper, and C. Kao (2001), hep-ph/0105182.

[197] E. Andres et al. (AMANDA) (1999), astro-ph/9906205.
[198] E. G. Anassontzis et al. (NESTOR), Nucl. Phys. Proc. Suppl. **85**, 153 (2000).
[199] E. Carmona (ANTARES), Nucl. Phys. Proc. Suppl. **95**, 161 (2001).
[200] M. Leuthold (1998), prepared for International Workshop on Simulations and Analysis Methods for Large Neutrino Telescopes, Zeuthen, Germany, 6-9 Jul 1998.
[201] M. Urban et al., Phys. Lett. **B293**, 149 (1992), hep-ph/9208255.
[202] V. S. Berezinsky, A. V. Gurevich, and K. P. Zybin, Phys. Lett. **B294**, 221 (1992).
[203] V. Berezinsky, A. Bottino, and G. Mignola, Phys. Lett. **B325**, 136 (1994), hep-ph/9402215.
[204] L. Bergstrom, P. Ullio, and J. H. Buckley, Astropart. Phys. **9**, 137 (1998), astro-ph/9712318.
[205] A. J. Tylka, Phys. Rev. Lett. **63**, 840 (1989).
[206] M. S. Turner and F. Wilczek, Phys. Rev. **D42**, 1001 (1990).
[207] M. Kamionkowski and M. S. Turner, Phys. Rev. **D43**, 1774 (1991).
[208] I. V. Moskalenko and A. W. Strong, Phys. Rev. **D60**, 063003 (1999), astro-ph/9905283.
[209] A. Barrau (AMS) (2001), astro-ph/0103493.
[210] G. L. Kane, L.-T. Wang, and J. D. Wells (2001), hep-ph/0108138.
[211] E. A. Baltz, J. Edsjo, K. Freese, and P. Gondolo (2001), astro-ph/0109318.
[212] J. Silk and A. Stebbins (1992), cFPA-TH-92-09.
[213] P. Chardonnet, G. Mignola, P. Salati, and R. Taillet, Phys. Lett. **B384**, 161 (1996), astro-ph/9606174.
[214] A. Bottino, F. Donato, N. Fornengo, and P. Salati, Phys. Rev. **D58**, 123503 (1998), astro-ph/9804137.
[215] F. Donato, N. Fornengo, and P. Salati, Phys. Rev. **D62**, 043003 (2000), hep-ph/9904481.
[216] Joint LEP 2 Supersymmetry Working Group, `http://lepsusy.web.cern.ch/lepsusy/Welcome.html`.
[217] K. T. Matchev and D. M. Pierce, Phys. Rev. **D60**, 075004 (1999), hep-ph/9904282.
[218] H. Baer, M. Drees, F. Paige, P. Quintana, and X. Tata, Phys. Rev. **D61**, 095007 (2000), hep-ph/9906233.
[219] V. D. Barger and C. Kao, Phys. Rev. **D60**, 115015 (1999), hep-ph/9811489.
[220] K. T. Matchev and D. M. Pierce, Phys. Lett. **B467**, 225 (1999), hep-ph/9907505.
[221] J. D. Lykken and K. T. Matchev, Phys. Rev. **D61**, 015001 (2000), hep-ph/9903238.
[222] R. Demina, J. D. Lykken, K. T. Matchev, and A. Nomerotski, Phys. Rev. **D62**, 035011 (2000), hep-ph/9910275.